Specific Ion Effects at the Air/Water Interface

Pavel Jungwirth*,† and Douglas J. Tobias*,‡

Institute of Organic Chemistry and Biochemistry, Academy of Sciences of the Czech Republic, and Center for Biomolecules and Complex Molecular Systems, Flemingovo nám. 2, 16610 Prague 6, Czech Republic, and Department of Chemistry and Institute for Surface and Interface Science, University of California, Irvine, California 92697-2025

Contents

1. Introduction

Aqueous ion-containing interfaces are ubiquitous and play a key role in a plethora of physical, chemical, atmospheric, and biological processes, from which we mention just a few illustrative examples: (i) Ions at the air/water interface are important for atmospheric chemistry involving ocean surfaces and seawater aerosols,[1–5] as well as that of the Arctic snowpack covered by sea spray.[6,7] (ii) Many salts (such as NaCl) tend to inhibit bubble coalescence,[8–12] which is one of the reasons why foam is formed when waves break in the ocean but not in freshwater lakes. (iii) Brine rejection occurring at the seawater/ice interface has profound climatic effects in polar regions.[13] (iv) The aqueous electrolyte/metal interface is involved in electrode and corrosion processes.[14,15] (v) Ion specificity plays an important role for interactions between colloid particles in electrolytes[16] and for the stability of aggregates of amphiphilic species, such as vesicles or micelles, in salt solutions.[17] (vi) Ions at the bio(macro)-molecule/water interface are crucial for protein stability,[18,19] to name at least one biological implication.

To cover specific ion effects at all possible aqueous interfaces would be an almost heroic endeavor. Our goal is more modest: we aim to focus on the simplest one, i.e., the air/water interface. The general atmospheric and technological importance of this interface alone justifies our selection. Moreover, interactions between ions and air or vapor are sufficiently weak so that the nonaqueous phase can often be viewed as a vacuum. Thus, all that remains to be explored are the structural and dynamical consequences of specific interactions between ions and water molecules within the inhomogeneous interfacial region. In the subsequent sections we attempt to review the rapidly expanding body of computer simulations of ions at the air/water interface. We focus on relatively small inorganic ions (which, according to the traditional, purely electrostatic picture, should actually always be repelled from the aqueous surface), leaving aside the huge body of literature concerning technologically very important organic ionic surfactants. We present the computational results in light of continuum models and, in particular, experimental observations, ranging from traditional surface tension measurements to modern surface selective photoelectron and nonlinear optical and vibrational spectroscopies, with the aim of capturing the emerging broader picture of ion specific behavior at the air/water interface.

To set the stage for the development of a molecular picture, we begin by considering the simplest physical picture of an ion at an aqueous interface, shown in Figure 1. Within this model the ion is fully characterized by the size of its charge q and radius R. The aqueous and nonaqueous media are treated as dielectric continua defined solely by their dielectric constants and separated from each other by an infinitely sharp and perfectly flat interface. The free energy change upon moving an ion from air (vacuum) to water is, within the crudest Born model,[20] given as $\Delta G = -(1 - 1/\epsilon)q^2/4\pi\epsilon_0 R$, where $\epsilon \approx 80$ is the dielectric constant of water and ϵ_0 is the permittivity of a vacuum. The large drop in energy upon ion hydration is thus the reason for the preference of the ions for the aqueous bulk.

A useful concept for understanding the solvation of ions at the water/low-dielectric medium interface is that of the image charge. It can be shown that an aqueous ion with charge q is effectively repelled from the air/water interface by a fictitious image charge $q' = q(\epsilon - 1)/(\epsilon + 1)$, i.e., which is of the same sign and practically the same value of charge (see Figure 1).[21,22] The energy profile connected with moving an ion from water to the low-dielectric phase (air in this case) is depicted in Figure 2.[23,24] Note that for a point charge the energy diverges at the infinitely sharp interface, while for finite ion radii the energy profile is continuous. Studies going beyond the model of an infinitely sharp flat interface have

* To whom correspondence should be addressed. P. J.: e-mail: pavel.jungwirth@uochb.cas.cz; phone, ++420-220410314; fax, ++420-220410320. D. J.T.: e-mail, dtobias@uci.edu; phone, ++1-9498244295; fax, ++1-9498248571.
† Academy of Sciences of the Czech Republic.
‡ University of California, Irvine.

Pavel Jungwirth graduated in physics from the Charles University in Prague in 1989. He completed his doctoral thesis in computational chemistry at the Heyrovský Institute in Prague under Rudolf Zahradník in 1993. In 1994–5 he was a Golda Meir Fellow at the Hebrew University in Jerusalem and a postdoc at the University of California at Irvine, working with Benny Gerber on quantum molecular dynamics of polyatomic systems. In 1995–2003 he was a research group leader at the Heyrovský Institute, and in 2004 he moved with his group to the Institute of Organic Chemistry and Biochemistry of the Academy of Sciences of the Czech Republic. Since 2000 he has also been an Associate Professor at the Charles University. In 2001 he was a Lady Davis visiting professor at the Hebrew University, and in the same year he was awarded the Annual Medal of the International Academy of Quantum Molecular Science. His current research interests encompass molecular simulations of ions at aqueous interfaces, chemistry of atmospheric aerosols, structure and dynamics of solvated and dipole bound electrons, and interactions of ions with biomolecules.

Doug Tobias received his B.S. and M.S. degrees in chemistry from the University of California, Riverside, and his Ph.D. in chemistry and biophysics from Carnegie Mellon University. Following appointments as a postdoctoral researcher at the University of Pennsylvania and guest researcher at the National Institute of Standards and Technology, in 1997 he joined the faculty in the department of chemistry at the University of California, Irvine. His research involves the application of molecular dynamics simulations to a wide variety of problems in biophysical and atmospheric chemistry, with an emphasis on structure and dynamics at interfaces.

shown that a nondiverging energy profile is also obtained for a smooth gradual interface between the two media,[25] and its shape is influenced by surface roughness.[26−28] A very important and often overlooked result is that a finite size ion can be brought to the interface from the water side with an energy cost that is only a fraction of the ion hydration energy, since a steep rise in energy only occurs at the air side of the interface. For example, it only takes about 3 kT to bring an ion of roughly the size of Na^+ (with hydration energy around 200 kT) from water to the interface (see Figure 2).[23] This relatively small increase in energy can still be
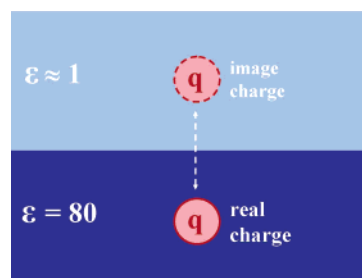

Figure 1. Continuum dielectric model of an ion at an aqueous interface. The ion is repelled from the interface into the aqueous phase by an "image" charge of the same size and polarity.
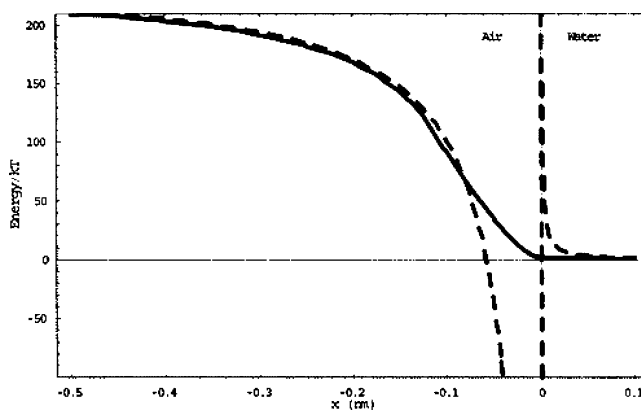

Figure 2. Energy profile of an ion moving across the air/water interface. Note the disappearance of the energy divergence at the interface upon the change from a point charge (dashed line) to a finite size sodium ion (full line). Also note that in the latter case the energy starts to steeply rise only after crossing the interface into the gas phase. The energy in the aqueous phase is arbitrarily set to zero. (Reprinted with permission from ref 23. Copyright 2002 American Chemical Society.)

sufficient to cause a significant depletion of ions from the aqueous interface, provided, however, that no other than Coulomb interactions come into play. One of the main goals of the present review is to explore these "other" ion specific interactions and the consequences thereof. Electrostatic forces, as described within the model of a charged sphere in a dielectric continuum, are of key importance, but they do not provide the whole picture. Such a model, e.g., does not distinguish between cation vs anion solvation, since it lacks specific ion−water interactions in the first solvation shell, as well as polarization and dispersion effects, and it also underestimates solvation entropy effects.[29,30] Polarization, dispersion, and solvophobic forces (the solvophobic effect being connected with the work necessary for creating the cavity to place the ion into the liquid[23]) can at least approximately be accounted for already within the continuum solvent framework. This is done to a varying extent in recent continuum models of ions at aqueous interfaces: as a result, ion specific behavior is inferred, including, in some cases, a propensity of certain types of ions for the air/water interface.[23,31−36]

Continuum models, however, should not be pushed beyond their range of validity, i.e., to effects at sub-nanometer separations where the "granularity" of the ion−water and water−water interactions is of key importance. This involves the first solvation shell structure, as well as the detailed behavior of ions at aqueous interfaces. Theoretical questions at the angstrom scale can hardly be properly addressed without calculations with atomic resolution. Statistically
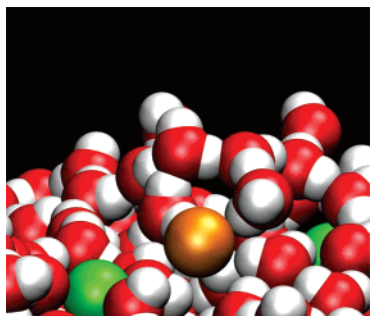
Figure 3. A cut from a snapshot from a molecular dynamics simulation of an aqueous salt solution/vapor interface demonstrating the atomic resolution of the obtained picture. The particular system shown here is NaBr(aq) with sodium in green and bromide in gold.

averaged results containing all the molecular details can be obtained by molecular dynamics (MD) or Monte Carlo (MC) simulations.[37] These simulations employ either an empirical force field (i.e., a prescribed interatomic interaction potential of an analytical form)[37] or the Car–Parrinello approach,[38] where forces are evaluated by quantum chemical methods such as the different variants of the density functional theory.[39] MD and MC calculations do not involve any macroscopic parameters (e.g., dielectric constants) but rather derive all properties from motions of mutually interacting atoms. An ion-containing aqueous interface within this picture is shown in Figure 3. This snapshot from a MD simulation demonstrates the atomic resolution one can obtain with all the details concerning ion distributions, molecular orientations, hydrogen bonding patterns, and surface corrugation accessible for analysis.

2. Historical Perspective and Previous Reviews

The research field of surfaces of electrolytes was flourishing in the first half of the 20th century, following the pioneering measurements of surface tension of aqueous salt solutions by Heydweiller in 1910.[40] The experimentally observed increase in surface tension upon adding salt was first theoretically addressed by Wagner[21] and Onsager and Samaras.[22] The surface tension increase was related via the Gibbs adsorption isotherm[41] to a depletion of ions from the interfacial layer, and an existence of a universal limiting law (in the spirit of the Debye–Hückel theory for bulk electrolytes[42]) was proposed. Ion specificity, i.e., the experimentally observed weak cationic but strong anionic specific effects on surface tension,[40,43,44] was only marginally dealt with in the early theoretical works. Despite that and despite the disturbing fact that strong monovalent acids (unlike salt and base solutions) actually decrease rather than increase surface tension,[43,44] for the next half-century the common wisdom largely continued to be based on these pioneering studies. This is reflected, e.g., in the classic book by Adam[45] and a series of two review articles by Randles[46,47] which all invoke an essentially ion-free and inert surface layer of aqueous salt solutions.

After a relatively long period of stagnation which followed the early boom, the 1990s marked the beginning of a renewed interest in surfaces of simple electrolytes. The presence of halogen anions at the air/water interface was inferred from laboratory measurements, motivated by an interest in atmospheric chemical processes, of the reactive uptake of molecular halogens on droplets of sodium halide solutions[1] and the kinetics of chloride oxidation in sea salt aerosol by

hydroxyl radical.[3] Also, the long-neglected problem of ion specificity at the air/water interface came into focus from the perspective of the Hofmeister series,[18,48] an old concept familiar to biochemists but historically largely ignored by physical chemists. Hofmeister ordered ions with respect to their efficiency to precipitate a given protein from an aqueous solution.[48] However, the importance of the series reaches far beyond salting-out of proteins, as demonstrated, e.g., in a recent special issue[34] reviewing Hofmeister effects in biochemical systems, in solutions, in colloids, and at the air/water interface.

Modern approaches to ion specificity at the air/water interface are threefold, based on surface selective experiments, theoretical continuum dielectric models, and molecular simulations. State-of-the-art experimental techniques probing the interfacial region of electrolyte solutions range from vibrational sum frequency generation spectroscopy (VSFG),[49–54] second harmonic generation spectroscopy (SHG),[55,56] and high-pressure VUV photoelectron spectroscopy,[57,58] to X-ray photoelectron spectroscopy combined with scanning electron microscopy (SEM),[2,59] ion sputtering,[60,61] and metastable impact electron spectroscopy (MIES)[62] (the last two methods investigate amorphous ice surfaces, while the one before probes deliquesced salt surfaces).

Contemporary theoretical approaches based on the continuum dielectric description of the aqueous solvents and the surfaces thereof go beyond the early Born-type model of Onsager and Samaras[22] and the Derjaguin–Landau–Verwet–Overbeek (DLVO) theory of colloids.[63,64] Ion specific effects, such as dispersion, polarization, solvophobicity, and first solvation shell effects, are accounted for to certain amounts and varying degrees of accuracy, as seen from several recent review and research articles.[23,31–33,35,36,65] Historically, the youngest approach to the problem of surfaces of electrolytes is via computer simulations with atomic resolution. Molecular dynamics simulations of extended solution/vapor interfaces were pioneered in the late 1980s and early 1990s[66–68] and partially reviewed in our 2002 Feature Article.[69] The present review not only significantly expands the scope of the previous summaries but also brings an up-to-date account of this thriving field of research at a point when it is reaching a new level of maturity. At the same time, we aim at providing a unified molecular picture of the air/solution interface of aqueous inorganic salts, acids, and bases.

3. Theoretical and Computational Results

3.1. Single Ions

Strictly speaking, single ions in extended aqueous systems do not exist. In any realistic experimental situation there is always a finite ion concentration. Moreover, macroscopic neutrality requires that the charge of one type of ions is compensated by counterions. Nevertheless, it makes a lot of sense to study theoretically the "infinite dilution limit", i.e., single ions in aqueous systems. In this way it is possible to investigate the genuine ion–water interactions and to abstract from counterion effects present at finite concentrations. Moreover, single ions interacting with water molecules can also be observed experimentally, albeit only in cluster systems.

3.1.1. Clusters

Historically, cluster simulations at ambient conditions (or at somewhat reduced temperatures in order to prevent rapid
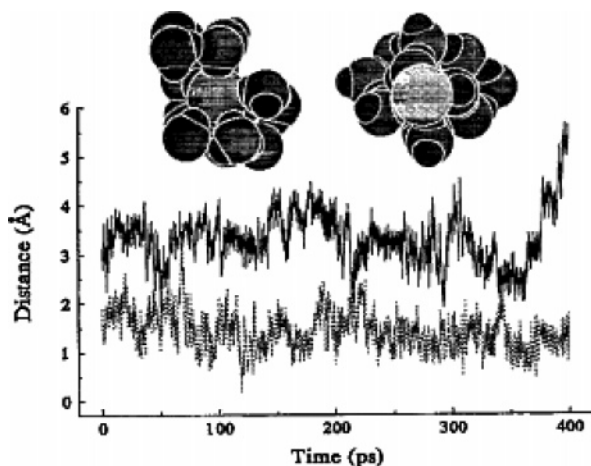
Figure 4. Time dependence of the distance to the chloride ion from the center of mass of the Cl$^-$(H$_2$0)$_{14}$ cluster in the SPCE/POL model (solid line) and in the TIP4P model (dotted line). Also shown are typical cluster configurations obtained from the SPCE/POL model (right: surface solvation) and from the TIP4P model (left: interior solvation). (Reprinted with permission from ref 74. Copyright 1993 American Institute of Physics.)

evaporation) of systems containing from several up to a few hundred water molecules were the first calculations to predict asymmetric (surface) aqueous solvation of certain ions such as the heavier halides, i.e., chloride, bromide, and iodide.[70-87] The first solvation shell of monovalent atomic ions typically contains around six water molecules. We, therefore, focus on clusters at and above this critical size, where the simulations can already start distinguishing between surface and interior ion solvation. A key ingredient of the above MD simulations for the surface propensity of the ion has been the use of polarizable force fields. Without polarization interactions, heavier halides prefer interior solvation in water clusters, similarly as in the case of, e.g., alkali cations. This is demonstrated in Figure 4, which shows the degree of asymmetricity of ion solvation by depicting distances of chloride from the center of mass of the cluster and snapshots from simulations with polarizable vs nonpolarizable force fields of a Cl$^-$(H$_2$O)$_{14}$ cluster.[87] A detailed analysis of the simulations shows that both ion and water polarizabilities contribute to the surface solvation of soft ions,[84,85,88] and so do the ionic size and to some extent also sign (anions being more easily accommodated at the surface than cations).[67,70,84] Finally, the entropy effects are non-negligible as well, although it is the enthalpy contribution that primarily determines the surface vs interior preference of a particular ion.[84] Predictions of asymmetric cluster solvation of large polarizable halides, as opposed to small nonpolarizable ions such as fluoride, sodium, or potassium which exhibit interior solvation, were verified by photoelectron spectroscopy measurements,[89,90] vibrational spectroscopy,[91] as well as electronic structure calculations[92-97] and ab initio molecular dynamics and Monte Carlo simulations.[98,99]

Asymmetric solvation in water clusters was also predicted for soft molecular inorganic anions such as nitrate and azide via quantum chemical and MD calculations, supported by photoelectron spectroscopy.[100-102] Using the same computational methods, another such soft anion, sulfate, was shown to solvate in the center of a water cluster,[103] in agreement with photoelectron spectroscopy measurements.[104,105] The reason for the preference of SO$_4^{2-}$ for the aqueous bulk is the multiplicity of the charge of the dianion. Consequently, electrostatic interactions, which favor bulk solvation and are

significantly stronger here than for monovalent ions, overwhelm the surface-driving polarization effects. A similar preference for the interior of water clusters was also observed for other doubly charged negative ions, such as the small dicarboxylate dianions from oxalate up to about adipate.[104] Larger dicarboxylate dianions, starting roughly with suberate, are accommodated, however, at the surface of water clusters.[106,107] In this case (as well as for other organic ionic surfactants), the surface driving force is the hydrophobic interaction of the aliphatic chain rather than polarization effects.

Last but not least, we mention the ionic product of water, i.e., the hydronium cation and hydroxide anion. The proton as a bare positive charge has the largest hydration energy among monovalent ions,[108] and its polarizability is by definition equal to zero. Therefore, it seems that it should solvate in the interior of water clusters similarly to the alkali cations. However, a hydrated proton readily forms transient chemical bonds with the surrounding water molecules. The classical (Eigen) form of hydronium is thus a H$_3$O$^+$ cation where each of the hydrogens is strongly bound to a water molecule, forming a H$_9$O$_4^+$ complex.[109] The proton can also be equally shared by two neighboring water molecules, forming the so-called Zundel cation H$_5$O$_2^+$.[110] In reality, a proton in an aqueous environment oscillates between these two extreme forms and also frequently (roughly every 1−2 ps) hops from one site to another.[111]

As a result of the above complex nature of the hydrated proton, a rigorous description requires a quantum mechanical description of both its electronic structure and nuclear dynamics.[112] However, classical molecular dynamics suffices in many cases, particularly for qualitatively or semiquantitatively answering structural questions which are the focus of this review. The most recent ab initio MD study employing B3LYP and BLYP functionals of a proton hydrated in large water clusters somewhat surprisingly shows that it prefers asymmetric surface solvation.[113] The main reason behind this is the amphiphilic nature of the hydronium cation, which can donate three strong hydrogen bonds but due to the small partial charge on the oxygen atom is a very bad hydrogen bond acceptor.[113] Therefore, hydronium prefers to be accommodated at the surface of a water cluster with oxygen pointing into the gas phase rather then disrupt the hydrogen bonding network inside the cluster. This behavior is also born out from high-level ab initio calculations, supported by photoelectron spectroscopy measurements, for a proton on water clusters including the "magic number" dodecahedral system, containing 21 water molecules.[114] A similar surface propensity of H$_3$O$^+$ is observed even using a carefully parametrized empirical polarizable potential,[115,116] while a simple nonpolarizable model did not seem to show an appreciable surface effect.[117,118]

For hydroxide anion, electronic quantum effects are important as well, since it forms as an acceptor very strong hydrogen bonds with an appreciable degree of charge transfer to three neighboring water molecules.[119] High-level ab initio calculations show that hydroxide solvates asymmetrically (similarly, e.g., to chloride) in clusters up to water hexamer.[120,121] Classical MD and Monte Carlo simulations of OH$^-$ in larger water clusters also show a weak tendency for asymmetric solvation, although the anion becomes rather delocalized within the cluster at higher temperature corresponding to the liquid state.[117,118,122]
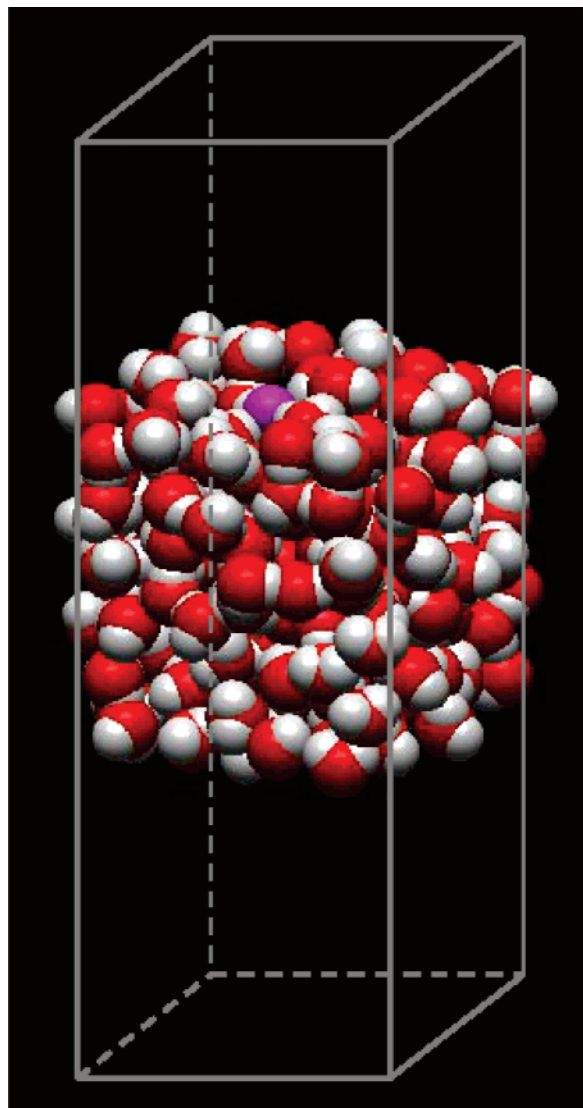
Figure 5. Prismatic unit cell with an aqueous slab containing a single ion.

3.1.2. Extended Interfaces

It is questionable how well a cluster surface can represent the extended surface of an electrolyte solution. Even at the current computational limit for classical MD simulations of about 10^5-10^6 atoms, the cluster is still very small (diameter on the order of tens of nanometers). At this size, the cluster surface is far from flat and curvature effects strongly influence macroscopic properties (such as surface tension) as well the distributions of ions within the cluster.[86] A simple computational trick that allows for moving from a finite size cluster to an extended water/vapor interface is the employment of a special type of periodic boundary conditions. The use of a standard (most often cubic) periodic unit cell leads to a simulation of a bulk region of the liquid, typically under constant-pressure conditions.[37] To model the interface, it is necessary to significantly extend one dimension of the box and run a constant-volume simulation.[66-68] For this prismatic unit cell, the aqueous system collapses into an infinite slab with two water/vapor interfaces, as depicted in Figure 5. More precisely, the use of 3D periodic boundary conditions results in a situation where the system comprises an infinite set of identical slabs, parallel to each other and separated from each other by a vapor region. For a sufficient elongation

of the unit prism (typically the largest box dimension should be at least twice or three times larger than the other two dimensions), the interactions between the slabs become small and one can use the fast 3D particle mesh Ewald approach[123] to account for long-range electrostatic interactions. This is demonstrated in Figure 6, which shows density profiles from a series of slab calculations for 1 M aqueous NaI. Parts a−c compare results employing 3D Ewald summation for two different elongations of the unit cell to a calculation employing a simple slab correction.[124] Within the statistical noise, the density profiles of iodide are the same in all three simulations and the sodium density profiles are also very similar to each other (see below for a detailed discussion of the surface propensity of iodide and other ions). This indicates that the periodicity in the direction perpendicular to the surface does not introduce any artifacts. The results for a simulation with the Ewald summation turned off (Figure 6d) are also similar to the previous ones, with the subtle differences in density profiles being due to the influence of the long-range electrostatics on the structure of the solution.

Another option to account for long-range electrostatic interactions in slabs is to employ 2D periodic boundary conditions. This has made the evaluation of the long-range electrostatic contribution computationally rather slow previously; however, there has been significant progress in efficient 2D Ewald algorithms recently.[125-130] Finally, note that, for a typically employed size of a prismatic unit cell of roughly $3 \times 3 \times 10$ nm^3 and for normal atmospheric pressure, there is only about one nitrogen or oxygen molecule per unit box. The effect of the gaseous phase on the interfacial ionic distributions is, therefore, negligible, and for the purpose of the present discussion, we can interchangeably talk about water/vapor and water/air interfaces.

The pioneering simulations of single ions in aqueous slabs did not show any propensity of ions for the air/water interface.[66-68] This was partially due to the choice of investigated ions, which, with the exception of chloride, encompassed only small hard ions (sodium and fluoride), and also due to the neglect of polarization interactions in the employed force fields. Nevertheless, already these early studies showed some ionic specificity with respect to the interface. For example, it was demonstrated that anions tend to penetrate closer to the surface than cations.[67]

The first slab simulations of ions at the air/water interface employing polarizable potentials appeared around the turn of the millennium, and consequently, the picture changed considerably.[3,86,131] A single polarizable chloride anion was shown in long, direct MD simulations to exhibit a weak surface propensity, maintaining an almost intact first solvation shell (while sodium cation continued to be repelled from the air/water interface).[86,131] In addition, an increasing surface propensity in the series Cl$^-$ < Br$^-$ < I$^-$ emerged from direct simulations of slabs containing concentrated aqueous salt solutions.[132] Shortly thereafter, the same effect was also shown by potential of mean force calculations, in which a single ion is moved in small steps across the slab and the corresponding free energy profile is evaluated.[133,134] Indeed, the free energy profiles of moving a single bromide or iodide from the aqueous bulk into the vapor phase across the air/water interface exhibit surface minima of around 1 kcal/mol, and chloride moves toward the surface without an appreciable barrier, provided polarizable potentials for ions and water are employed.[133,134] Figure 7 shows the free energy profiles
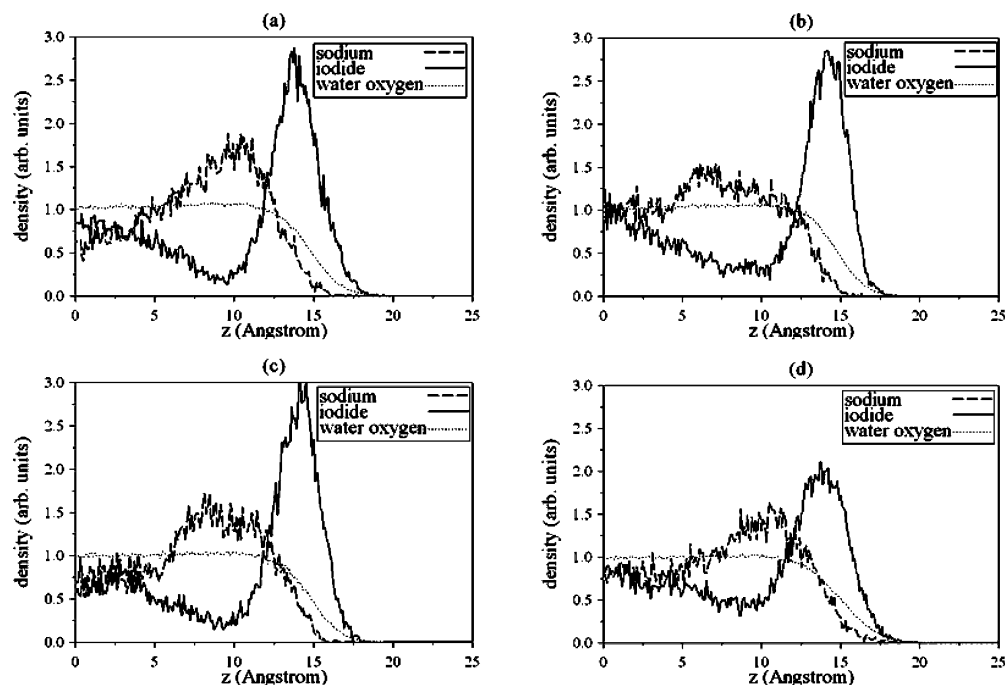
Figure 6. Density profiles (i.e., abundancies of individual species in layers parallel to the surface, from the center of the slab across the interface to the gas phase) from 1 ns slab simulations of 1 M aqueous NaI employing (a) 3D Ewald summation with a unit cell of $3 \times 3 \times 10$ nm^3, (b) 3D Ewald summation with a unit cell of $3 \times 3 \times 20$ nm^3, (c) 3D Ewald summation with a slab correction[124] employing a $3 \times 3 \times 10$ nm^3 unit cell, and (d) a simulation employing a $3 \times 3 \times 10$ nm^3 unit cell with Ewald summation turned off (employing a cutoff of 1.2 nm).
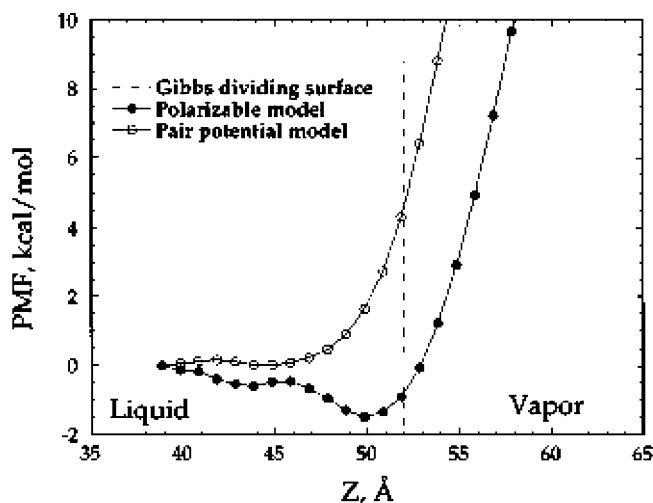

Figure 7. Free energy profile (potential of mean force) associated with moving iodide from the center of an aqueous slab across the air/water interface at 300 K. Note that a surface minimum only develops for a polarizable potential model. (Reprinted with permission from ref 133. Copyright 2002 American Chemical Society.)

of moving an iodide anion from the aqueous bulk across the air/water interface calculated using polarizable and nonpolarizable force fields.[133] We see that only in the former case does a surface free energy minimum, which is directly related to the enhancement of I$^-$ at the surface, develop.

The effect of ion polarizability on the surface propensity can be in a simplified and somewhat schematic way rationalized as follows. While in the bulk, the water environment around an ion is roughly symmetric and, consequently, the electric field created by the vector sum of the water dipoles and acting on the ion is relatively small. At the surface, however, the environment is asymmetric and, as a result, the resulting large solvent electric field strongly polarizes the ion.[88] Similarly, polarization of the solvent

molecules also plays a role here.[84,88] For a sufficiently soft ion, this polarization stabilization can compensate much of the electrostatic penalty due to a partial loss of solvation, leading in the end to a surface affinity. Of course, the situation drawn here represents necessarily an oversimplified qualitative picture which neglects, e.g., the surface roughness of an aqueous solution; however, it is at least qualitatively supported by the simulations (for a representative snapshot of a bulk vs surface solvated chloride see Figure 8).

Recently, a similar surface propensity to that for heavier halides was also observed for a single nitrate or azide anion in a water slab,[101,102] while another soft inorganic molecular ion, sulfate, was shown to strongly favor interior solvation.[103] As in the clusters, the multiple charge on the latter ion is responsible for the preference of bulk solvation.

Simulations of a single hydronium cation in a water slab have been performed recently using a polarizable force field, as well as an empirical valence-bond approach which allows for proton hopping.[115,116,135] Calculations based on the potential of mean force methodology showed that hydronium can penetrate much closer to the aqueous surface than other small cations such as sodium.[115] Direct simulations employing both potential models mentioned above showed a strong preference of the hydrated proton for the air/water interface,[116,135] similarly as in water clusters. Figure 9 depicts a representative snapshot from a simulation showing a surface located single hydronium cation with oxygen pointing into the gas phase and hydrogens exhibiting strong hydrogen bonds with neighboring water molecules.[116] On the other hand, classical polarizable MD simulations of a single hydroxide in a water slab indicate a much weaker (if any) surface propensity of OH$^-$ than that observed in small clusters.[136]

While the extended air/water interface clearly differs from the surface of a finite size water cluster, where curvature effects are important (leading, for example, to a significant
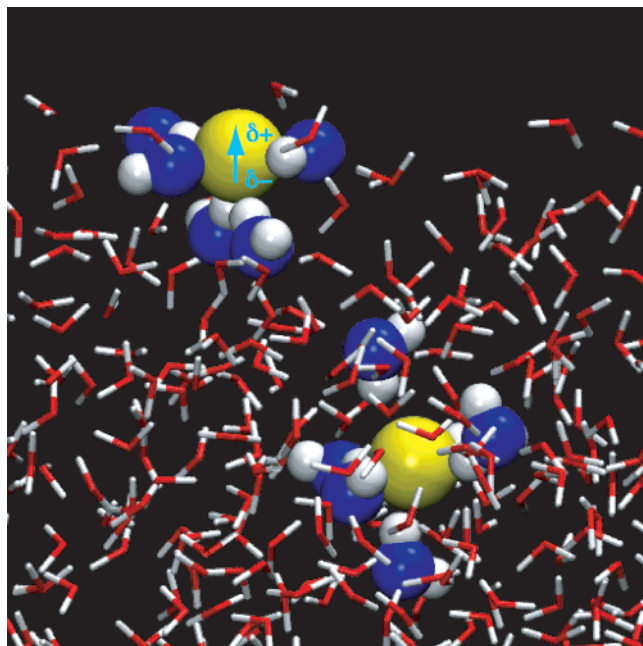
Figure 8. Snapshot from a molecular dynamics simulation of an aqueous chloride solution depicting two chloride anions and their first solvation shells in the van der Waals sphere representation. The anion in the lower right portion of the image is in the bulk interior of the solution and has a spherically symmetric solvation shell, on average. The anion in the upper left is undercoordinated at the solution/air interface. The asymmetric, incomplete solvation shell induces a sizable dipole on the anion at the interface.
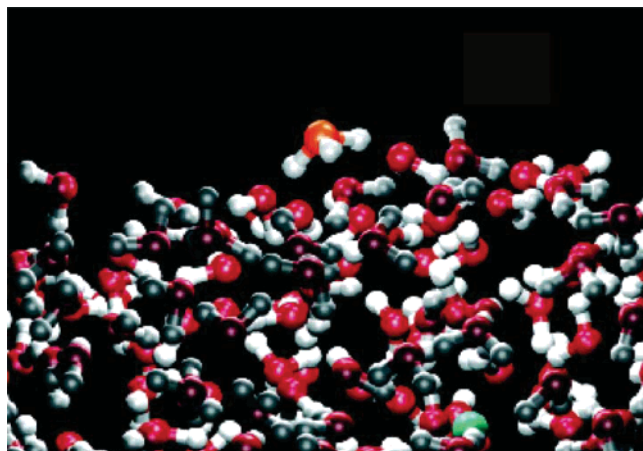

Figure 9. Representative structure from an effective valence bond MD simulation of a hydronium cation on an aqueous slab. (Reprinted with permission from ref 116. Copyright 2004 American Chemical Society.)

reduction in surface tension),[86] there is some correlation between the two environments in terms of surface vs bulk preference of host ions. However, one should keep in mind that there are significant quantitative and, in some cases, even qualitative differences and that, generally, the ionic surface propensity tends to be stronger in clusters than that in extended slabs.[86] Moreover, some of the cluster calculations are performed at very low temperatures where the system is more solidlike than liquidlike. In that case, the ions could be found at the surface solely for the simple reason that they were excluded from the interior of the ice nanoparticle by a microscopic analogy of the well-known brine rejection process.[13,137]

3.2. Finite Ion Concentrations and Counterion Effects

There are several merits to straightforward calculations of distributions of ions at extended air/solution interfaces of aqueous electrolytes. First, the finite amount of ions directly reflects the experimental reality of surfaces of electrolytes with typical concentrations up to several moles per liter. Second, finite concentration and counterion effects, which can play an important role at the air/solution interface, are directly modeled. Third, from the technical point of view, using an appreciable amount of ions significantly improves the statistics of the simulation and allows evaluating distributions of ions at the air/water interface, as well as macroscopic measurables, such as the changes in surface tension with respect to neat water. Provided that the free energy difference between bulk and interfacial ionic solvation is relatively small (of the order of several kT), a direct and sufficiently long simulation of a concentrated aqueous slab gives converged distributions of the individual ionic species in the whole interfacial layer. This turns out to be true for practically all simple inorganic ions.

Several classical and ab initio molecular dynamics and Monte Carlo studies of concentrated aqueous bulk solutions of simple inorganic salts, acids, and bases have been performed recently.[138−143] However, only after our first MD simulations of slabs containing concentrated salt solutions[3,69,131,132] has such a computational approach become established also for investigating air/solution interfaces.[88,135,144−146] Two ingredients of the simulations proved to be of crucial importance: (i) the inclusion of polarization interactions, which turned out to be responsible for a substantial part of the ionic surface propensity, and (ii) the employment of finite (typically molar) ion concentrations, which not only reflected the usual experimental reality but also allowed for statistically relevant direct sampling of the distribution of ions across the aqueous slab.

The first simulations of this type were performed for simple inorganic salt solutions for which the application of a classical force field is more straightforward than that for the corresponding acid or base solutions. The results of MD slab simulations of 1.2 M aqueous solutions of the sodium halide series are summarized in Figure 10.[132] While in the NaF solution both ions are, in agreement with common wisdom,[22,46,47] repelled from the air/water interface, leaving an almost ion-free top layer, none of the heavier halides behaves in accord with the standard theory of the surfaces of electrolytes.[22] Namely, chloride penetrates all the way to the interface and bromide and iodide even exhibit a surface concentration peak followed by subsurface depletion. Anions in the topmost layer are not completely solvated, but they do maintain a substantial solvation shell; for example, the ratio of the number of water molecules in the first solvation shell on the surface vs in the bulk is 4:6.2, 4.5:6.8, and 4.7:7.8, for chloride, bromide, and iodide, respectively (unpublished results from the simulations reported in ref 132). Note that the anion coordination number rapidly increases with depth below the surface, so that the average coordination number in the inhomogeneous interfacial region is close to the bulk value.[69]

As shown in detail recently, the surface propensity of heavier halides is due to several factors, out of which the ion and water polarizability and ion size dominate.[84,85,88] In terms of getting an anion to the surface of a solution, polarizability seems to be the most important factor, but size
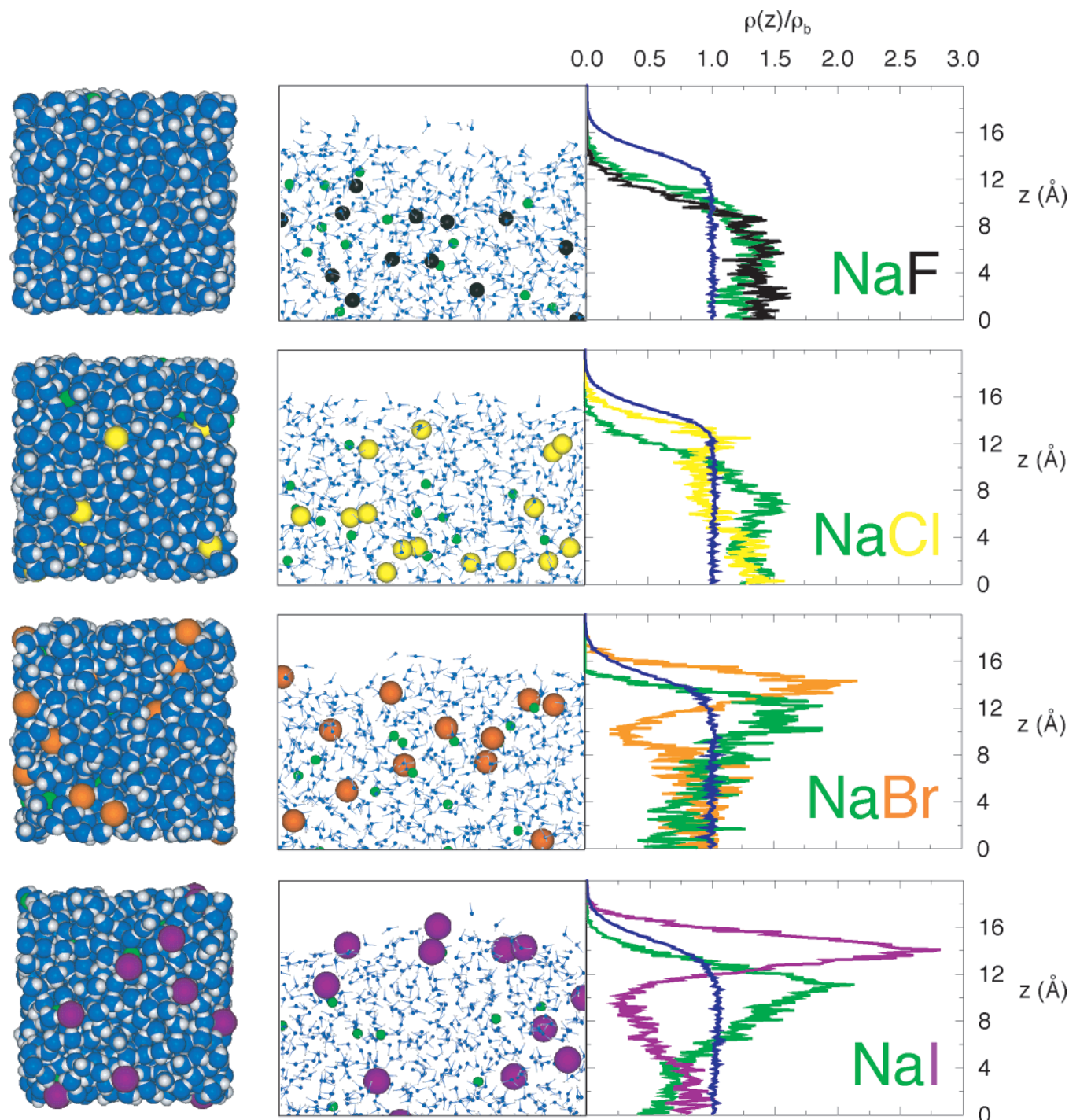
Figure 10. Snapshots (top and side views) of the solution/air interfaces of 1.2 M aqueous sodium halides from the molecular dynamics simulations and density profiles (number densities) of water oxygen atoms and ions plotted vs distance from the center of the slabs in the direction normal to the interface, normalized by the bulk water density.[132]

appears to be essential as well for the full surfactant-like behavior of strongly adsorbing anions such as iodide. The surface neutrality requirement demonstrates itself by the fact that, for the heavier halide solutions, the sodium cations are dragged by the anions toward the interface and, consequently, exhibit a subsurface peak. At the same time, the surface propensity of the heavier halides is somewhat weaker in concentrated solutions than at infinite dilution, where no counterion effects come into play.[133,147] This effect, which is primarily due to crowding and mutual repulsion of anions at the aqueous surface, e.g., reduces the surface peak of

thiocyanate by about 25% upon increasing the concentration of aqueous NaSCN from 0.6 to 3.2 M.[147]

The correspondence between the "virtual reality" of the MD simulations and surface tension and surface selective spectroscopic measurements is discussed in detail in the following section. Here, we touch upon the issue of the internal consistency of the simulations, particularly with respect to the employed interaction potential. How much can one rely on a simple, albeit polarizable force field, such as the three-site POL3[148] or four-site DC97[149] and TIP4P-FQ[150] water models combined with polarizable ions?[72,134,150,151] A
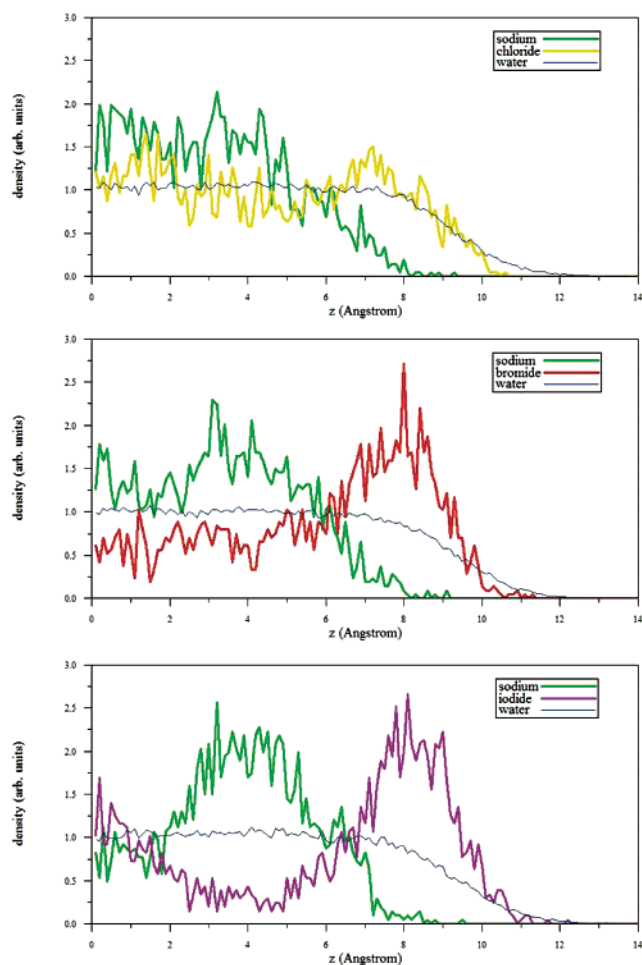
Figure 11. Density profiles of water oxygen atoms and ions for 1 M NaCl, NaBr, and NaI solutions obtained using the Amoeba force field.[158]

straightforward check of the empirical potential can be done via comparison of structures and energetics of small ion−water clusters against high-quality quantum chemistry calculations and ab initio molecular dynamics. This benchmarking turns out to be favorable for the above polarizable force fields, while nonpolarizable potentials tend to be inferior in many respects. For example, the former but not the latter potentials predict the correct asymmetric structure of the $Cl^-(H_2O)_6$ cluster with surface solvated chloride anion.[97,98] Generally speaking, nonpolarizable potentials fail to predict appreciable surface propensities of soft anions.[67,146]

Recently, a new generation of polarizable water models appeared. These potentials combine a more complex functional form with careful fitting to a large set of experimental and theoretical data. Typical representatives of these water potentials are the TTM2,[152] POL5/QZ,[153] SAPT,[154] VRT-(ASP-W),[155] and Amoeba[156] models. The last one is particularly suitable for the purpose of testing the results of previous MD simulations, since it also contains a consistent parametrization of alkali cations and halide anions.[157] The results of ion partitioning at the interface of 1 M solutions of NaCl, NaBr, and NaI simulated using the Amoeba potentials are presented in Figure 11.[158] Despite the somewhat inferior statistics (calculations with the Amoeba force field are computationally very demanding; therefore, a smaller slab system and shorter simulation times were employed), the results quantitatively agree with those obtained previously.[132]

In particular, the increasing anionic surface propensity in the series $Cl^- < Br^- < I^-$ is very well reproduced.

A similar surface propensity to that for heavier halides has also been observed in MD simulations of several soft monovalent inorganic molecular anions. From the technical point of view, constructing a polarizable force field for molecular ions is more complicated than that of atomic ions. Most MD programs employ isotropic atomic polarizabilities; therefore, molecular polarizability has to be cast into atomic contributions and possible effects of the polarization anisotropy should be considered. Within the force field parametrization, the polarizability of the isolated molecular ion is evaluated by ab initio methods (typically at the MP2 level with a sufficiently flexible basis set) and it is desirable to at least approximately account for the solvent effect, e.g., by replacing surrounding water molecules by fractional charges using geometries from an MD simulation or employing a continuum solvation model.[101,159,160] Note that the aqueous environment reduces the ionic polarizability by ∼5−25%, depending on the particular ion.[101,103,161] Of the molecular anions studied so far, most exhibit an appreciable surface propensity, with a good example being thiocyanate.[147] Sulfate salts, however, do not show any presence of ions at the air/water interface despite the fact that SO_4^{2-} is more polarizable than, e.g., iodide.[144] As already mentioned in the previous subsection, the strong bulk driving electrostatic forces overwhelm the surface-favoring polarization interactions for this (as well as other) multiply charged inorganic anion. The strong Coulomb interactions of multiply charged ions also tend to structure the ion free surface layer, which is broader than that, e.g., for solutions of monovalent surface-repelled ions, such as aqueous NaF.[144]

Most recently, classical MD simulations employing a simple polarizable force field have also been performed for slabs containing concentrated aqueous solutions of strong inorganic acids such as HCl, HBr, and HI, as well as a typical base such as NaOH.[135] This simple force field approach can neither describe quantum nuclear effects such as proton hopping nor quantitatively account for electronic delocalization and charge transfer within the very strong hydrogen bonds between water molecules and the hydroxide anion or hydronium cation. Nevertheless, the segregation of ions at the air/solution interface seems to be at least semiquantitatively described. A composite Figure 12 showing snapshots and density profiles summarizes the interfacial ionic behavior for a typical acid (HCl), base (NaOH), and salt (NaCl) aqueous solution at a molar concentration. We see a prominent difference between acids on one side and salts and bases on the other side. While, for acids, both cations (hydronium) and anions (chlorides) exhibit an affinity for the air/solution interface, in salts and bases, cations (sodiums) are repelled from the surface and anions show either a surface propensity (chlorides) or weak surface repulsion (hydroxides).[135] Important practical consequences of this difference between acids on one hand and salts and bases on the other hand are discussed toward the end of this review.

4. Experimental Studies and Comparison with Simulation Results

The central theme of this review is the specificity of the adsorption behavior of ions at the air/water interface. It has become apparent that some inorganic ions adsorb while others do not, and the principles that determine whether a given ion adsorbs are beginning to be well understood. The
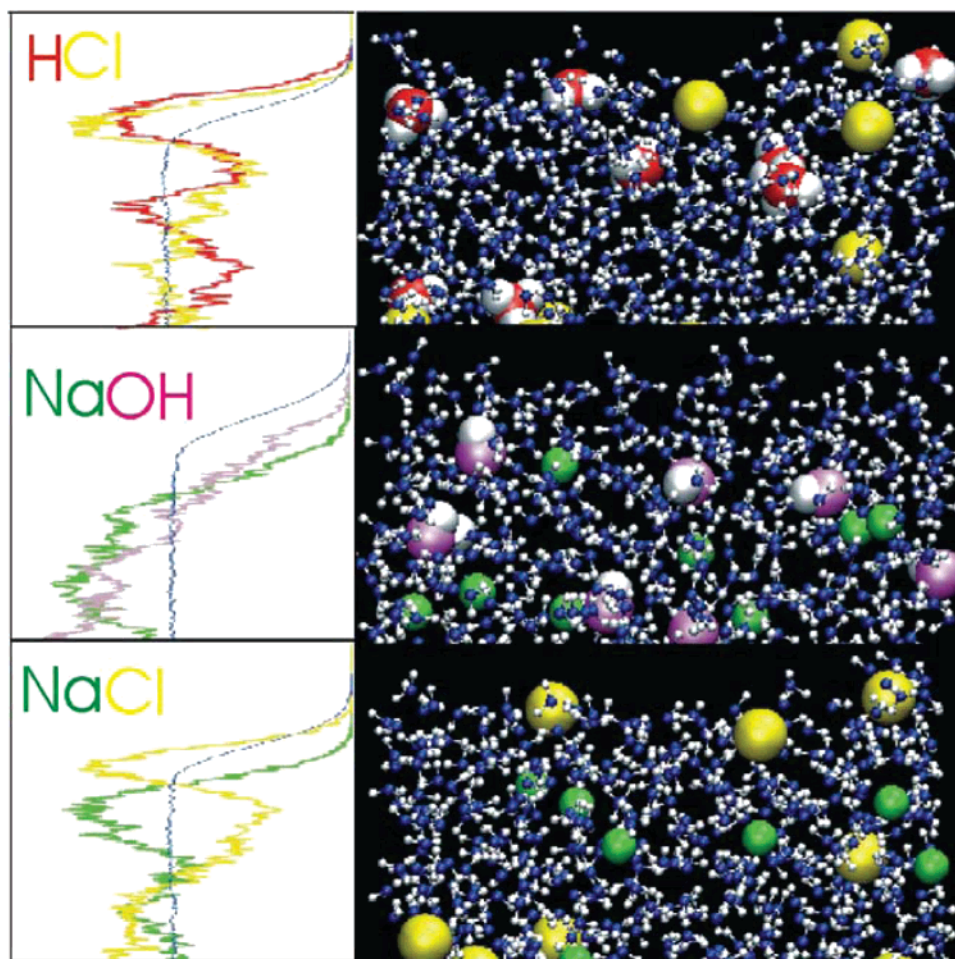
Figure 12. Density profiles and snapshots from MD simulations of 1.2 M HCl, NaOH, and NaCl.[135]

idea that some inorganic ions exhibit a propensity for the aqueous surface is only a few years old. For most of the last century, it was universally accepted that inorganic ions are repelled from the air/water interface. In this section we review the data from a wide variety of experiments and related results from MD simulations that have contributed to the evolution of our understanding of the interfacial properties of electrolyte solutions. We begin with the measurements and thermodynamic theory of surface tension that largely established the "old view" of an ion-free interface and allowed it to persist for decades. We then end up reviewing recent state-of-the-art spectroscopic measurements that appear to confirm the "new view" that some inorganic ions adsorb to the air/water interface and that there is considerable ion specificity in the adsorption behavior, as predicted initially by MD simulations over the last five years.

4.1. Surface Tension

We start with a brief review of the thermodynamic theory of surface tension since it is a cornerstone of the widely used practice of inferring interfacial composition from surface tension and because we will refer to it when reconciling surface tension data with the seemingly contradictory predictions of MD simulations. The thermodynamic theory of interfaces developed by Gibbs[41] and expanded subsequently by many others (see, for example, refs 45, 162−164) applies to interfaces between distinct phases containing an arbitrary number of components at equilibrium. Here we restrict our attention to the liquid/vapor interface and, to simplify the notation, we consider a system with only two components: a solvent (referred to as component 1) and a solute (referred to as component 2). Moreover, we assume that both components have negligible densities in the vapor phase. Thus, the description will be appropriate for ionic species or strongly polar molecules dissolved in water.

We consider a system with cylindrical symmetry, with the boundary between the two phases ($\alpha =$ liquid and $\beta =$ vapor) placed perpendicular to the cylinder axis. The separation between the phases is in reality an inhomogeneous region of a finite width. To develop his thermodynamic theory of interfaces, Gibbs introduced a model in which the interface is defined by a plane parallel to and within or near the inhomogeneous region. Once this fictitious "dividing surface" has been defined, it is possible to develop the thermodynamic theory of the interface in terms of surface excess quantities defined as the difference between the quantities in the entire system and the model system in which the liquid and gas phases extend right up to the dividing surface. One of the most important consequences is the Gibbs−Duhem equation for the surface, known as the Gibbs adsorption equation, which for two components at constant temperature and pressure of the whole system reads

$$A\,d\gamma + S^s\,dT + n_1^s\,d\mu_1 + n_2^s\,d\mu_2 = 0 \qquad (1)$$

Here A is the area of the dividing surface, γ is the surface tension, T is the temperature, μ_i is the chemical potential of species i, and S^s and n_i^s are, respectively, the excess entropy

and excess number of moles of species i. The latter quantities are defined by

$$n_i^s = n_i^t - n_i^\alpha - n_i^\beta \tag{2}$$

$$S^s = S^t - S^\alpha - S^\beta \tag{3}$$

where the superscripts t, α, and β refer to quantities in the whole system and in the α and β phases, respectively. Dividing eq 1 by A, and imposing constant T, we obtain the following equation, commonly referred to as the Gibbs adsorption isotherm:

$$d\gamma = -\Gamma_1 \, d\mu_1 - \Gamma_2 \, d\mu_2 \tag{4}$$

Here $\Gamma_i = n_i^s/A$, what Gibbs called the superficial density, now referred to as the Gibbs surface excess of species i. Note that according to eqs 2 and 4, Γ_i can be positive, zero, or negative, depending on the system and the choice of the location of the dividing surface (for a detailed analysis, see ref 164). Thus, at this point, the composition of the interface is not well defined due to the arbitrariness of the location of the dividing surface.

Gibbs pointed out that the dividing surface could be located at the point that makes $n_1^t = n_1^\alpha + n_1^\beta$, so that $n_1^s = 0$ and $\Gamma_1 = 0$. Then eq 4 becomes

$$d\gamma = -\Gamma_2^1 \, d\mu_2 \tag{5}$$

where Γ_2^1, referred to as the relative surface excess, is the excess amount of component 2 adsorbed at the particular surface where the excess of component 1 is zero. This choice is known as the Gibbs dividing surface. Γ_2^1 is a measure of the interfacial composition since, according to eq 5,

$$\Gamma_2^1 = \frac{-1}{RT}\left(\frac{\partial \gamma}{\partial \ln a_2}\right)_T \tag{6}$$

where a_2 is the activity (or concentration in the case of dilute solutions) of component 2. It may be shown (see, for example, ref 162) that, in the case where the amount of solute in the vapor (phase β) is negligible,

$$\Gamma_2^1 = \frac{1}{A}\left(n_2^t - n_1^t \frac{n_2^\alpha}{n_1^\alpha}\right) \tag{7}$$

This equation provides a basis for interpreting Γ_2^1, the excess at the hypothetical but well-defined Gibbs dividing surface, in terms of properties of the liquid phase of the real system.

Chattoraj[163] has made the interpretation more illuminating by defining the absolute amount of species i, Δn_i, in the inhomogeneous region of the real system via

$$n_i^t = n_i^\alpha + n_i^\beta + \Delta n_i \tag{8}$$

where indices α and β refer to homogeneous liquid and vapor regions. Hence, eq 7 becomes, for the case where the vapor may be neglected,

$$\Gamma_2^1 = \frac{1}{A}\left(\Delta n_2 - \Delta n_1 \frac{n_2^\alpha}{n_1^\alpha}\right) \tag{9}$$

Note that by definition Δn_i must be greater than or equal to zero, in contrast to the n_i^s defined in eq 2, which can also be negative. The quantity $\Delta n_2 - \Delta n_1(n_2^\alpha/n_1^\alpha)$ is the excess amount (relative to the bulk liquid phase α) of component 2 associated with Δn_1 mole of component 1 in the interfacial region, and it (and, hence, Γ_2^1) may be positive or negative. When component 1 is the solvent, a positive relative surface excess Γ_2^1 of component 2 means that there is a greater amount of component 2 (per unit area) associated with a given amount of solvent in the interfacial region vs the bulk, i.e., there is an enhancement of component 2 in the interfacial region. Conversely, a negative Γ_2^1 means that there is a depletion of component 2 in the interfacial region. The above approach can be readily extended to systems containing more than two components. Note that for an aqueous solution of a single strong electrolyte, which contains three components (i.e., water, cations, and anions), the surface neutrality condition comes into play, too.

The two above scenarios are illustrated in Figure 13 by surface tension vs concentration data and snapshots from MD simulations depicting the conventional interpretation of the corresponding Gibbs surface excesses. The surface tension of aqueous solutions of amphiphilic organic substances decreases with increasing concentration (Figure 13a), giving a positive Gibbs surface excess according to eq 6. This may be interpreted according to eq 9 as an enhancement of solute concentration in the interfacial region, i.e., as surfactant behavior (Figure 13b). In contrast, the inorganic salts, exemplified by the alkali halide data plotted in Figure 13c, increase the surface tension of the solution/air interface. Qualitatively, this corresponds to a negative Gibbs surface excess, i.e., a net depletion of the solute in the interfacial region, and this is usually taken as an indication that the ions are repelled from the interface, leaving an ion-free region at the interface (Figure 13d). This physical picture has been firmly in place since it formed the basis of the continuum theory advanced by Wagner[21] in 1924 following the first measurements of the surface tension of salt solutions by Heydweiller[40] in 1910, and it has persisted in the numerous refinements to Wagner's theory that followed, including the famous paper by Onsager and Samaras.[22]

A quantitative analysis based on eq 9 (i.e., making use of the linear dependence of Γ_2^1 on n_2^α/n_1^α) has afforded values of Δn_1 on the order of 10^{-9} mol/cm^2 and $\Delta n_2 \approx 0$ for 1:1 electrolytes.[163] On the basis of this analysis, it was concluded that a negligible amount of electrolyte is associated with the interfacial water. Using reasonable geometric parameters for a water molecule, the corresponding number of layers of water molecules constituting the ion-free interfacial zone was estimated to be between 0.9 and 1.7.[163]

The data shown in Figure 13c show that, while the surface excess is not very sensitive to the identity of the (monovalent) cation, it is anion specific, decreasing (i.e., increasing in absolute value but becoming more negative) in the order I$^-$ > Br$^-$ > Cl$^-$ > F$^-$. Thus, the depletion of ions in the interfacial region increases in the order I$^-$ < Br$^-$ < Cl$^-$ < F$^-$. A similar analysis of the data plotted in Figure 14 suggests that the interface of strong base solutions is depleted of ions, similar to the alkali halide salt solutions, while strong acid solutions contain surface active species (i.e., the surface tension decrease with concentration implies a positive surface excess) and, hence, are qualitatively different from the bases and salts.
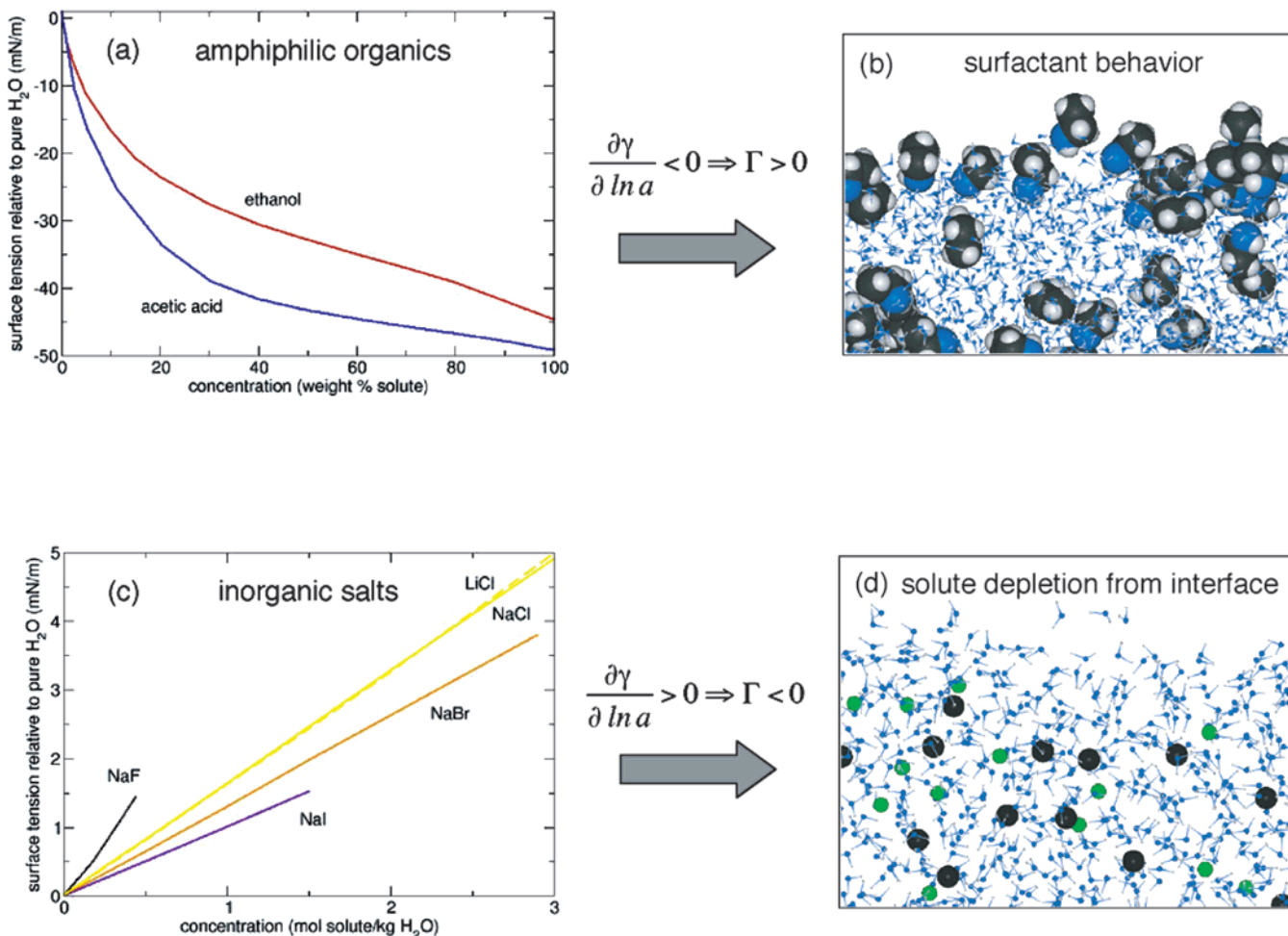
$$\frac{\partial \gamma}{\partial \ln a} < 0 \Rightarrow \Gamma > 0$$

$$\frac{\partial \gamma}{\partial \ln a} > 0 \Rightarrow \Gamma < 0$$

Figure 13. Surface tension vs concentration data for aqueous solutions of (a) amphiphilic organic molecules and (b) alkali halide salts. All of the surface tension data were taken from ref 43 except for the surface tensions of NaF solutions, which were taken from ref 202. Snapshots from MD simulations depicting the conventional interpretation of the corresponding Gibbs surface excesses are shown in part c for the surface of an ethanol/water solution and in part d for the surface of an aqueous solution of NaF.
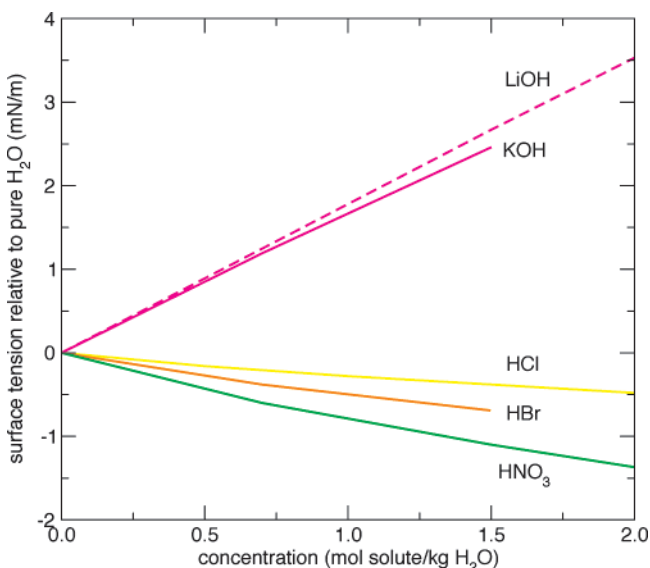

Figure 14. Concentration dependence of surface tension for aqueous acid and base solutions.[43]

Inferring interfacial composition from surface excesses determined by the concentration dependence of the surface tension, as exemplified for a few systems here, has been common practice in countless applications for many decades. However, it is important to keep in mind that the interfacial region is not an idealized planar surface and that the excess is defined over the entire inhomogeneous interfacial region, which may extend for a few to many molecular diameters, depending on the system. In the case of electrolyte/air interfaces, oscillations in solute concentrations within the finite dimension of the interface have important consequences for the microscopic interpretation of the surface excess. With the benefit of simulation data, we shall see that in the case of electrolyte solutions the surface excess does not always tell the whole story.

The microscopic theory of surface tension (see, for example, ref 165), embodied in eq 10 below provides a basis for computing the surface tension from a MD simulation:

$$\gamma = \int_{z_\alpha}^{z_\beta} [p_N(z) - p_T(z)] \, dz \qquad (10)$$

Here z is a coordinate along the surface normal, z_α and z_β are points in the bulk α and β phases, respectively, p_N is the component of the pressure tensor that is normal to the interface, and p_T is the tangential component. For a planar interface in the xy plane, $p_N(z) = p_N = $ constant for mechanical stability. In the case of a simulation of an

interfacial system in a slab geometry (Figure 5), eq 10 becomes

$$\gamma = \frac{1}{2}L_z\left\langle P_{zz} - \frac{1}{2}(P_{xx} + P_{yy})\right\rangle \quad (11)$$

where L_z is the length of the box in the z direction, the P_{ii} are the diagonal components of the pressure tensor, the angular brackets denote a time average, and the prefactor of $\frac{1}{2}$ accounts for the presence of two interfaces in the slab. For the sizes of systems typical for current solution simulations in the slab geometry, the fluctuations in the components of the pressure tensor produce statistical uncertainties in the surface tension in the range of one to several millinewtons per meter.

Surface tensions computed from MD simulations using eq 11 have been reported for a variety of electrolyte solutions in several recent papers. We performed simulations of 1.2 M solutions of the sodium halide series using polarizable force fields[132] and found that the surface tensions of all of the solutions were greater than that of neat water, and that the order of increase was NaI < NaBr < NaCl < NaF, in good agreement with the experimental data plotted in Figure 13. However, the same simulations predicted that the concentration of the heavier halides (Br⁻ and I⁻) on the surface of the solution was greater than that in the bulk (see Figure 10), in seeming contradiction to the Gibbs adsorption analysis. This important point, which has been considered a potential stumbling block in the advancement of the "new view" of salt interfaces,[166] will be discussed further below.

Bhatt et al. have compared the concentration dependence of the surface tensions of alkali halide solutions computed from MD simulations.[145,146] Their simulations employed nonpolarizable models including explicit water for NaF, NaCl, and NaBr solutions and a continuum solvent model for NaF and NaCl. For the most part, they found that the surface tension of the solutions was greater than that of neat water, in qualitative agreement with experimental data. The simulations employing the explicit solvent model gave the correct order of increase, namely NaBr < NaCl < NaF, while the continuum model incorrectly predicted that the surface tension of NaCl was greater than that of NaF over a wide concentration range. Direct calculation of surface excesses via density profiles from explicit solvent simulations of NaCl and NaBr solutions gave negative values at some concentrations and positive values at others and was consistent with the nonmonotonic increase in the computed surface tensions with concentration. The density profiles of Bhatt et al.[145,146] clearly indicated that both the anions and cations are repelled from interfaces, consistent with previous simulations employing nonpolarizable force fields[66−68] but in qualitative disagreement with simulations employing polarizable force fields.

As was discussed above in section 3.1.1, the superiority of polarizable force fields has been firmly established by their ability to correctly predict the surface location of the heavier halide anions on water clusters observed unambiguously in numerous experiments, as opposed to the qualitatively incorrect interior location predicted by nonpolarizable force fields. However, the adsorption of the heavier halides to the air/solution interface must be reconciled with the indisputable negative Gibbs excess associated with the surface tension increase.

Our simulations suggest two scenarios that are consistent with a negative Gibbs excess.[88] This may be seen by writing
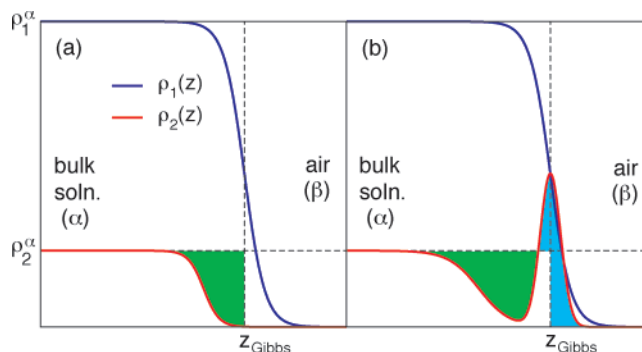

Figure 15. Schematic density profiles depicting the determination of Gibbs surface excesses from ion density profiles. The blue curves are the density profiles of water (component 1), and the red curves are the density profiles of an anion (component 2). The vertical dashed lines indicate the position of the Gibbs dividing surface, and the horizontal dashed lines indicate the anion densities in the bulk solution. The case of anion repulsion from the interface (e.g. F⁻) is shown in part a, and the case of an oscillatory density profile with a surfactant layer on the surface and a subsurface depletion zone (e.g. Br⁻, I⁻) is shown in part b. The areas shaded green give negative contributions to the Gibbs surface excess, and the area shaded cyan gives a positive contribution (see text).

Gibbs' definition of the relative surface excess of solute component 2, using eq 2 for n_2^s, in terms of density profiles (e.g., the quantities plotted in Figure 10):

$$\Gamma_2^1 = \int_{-\infty}^{\infty}\rho_2(z)\,\mathrm{d}z - \rho_2^\alpha\int_{-\infty}^{z_{Gibbs}}\mathrm{d}z - \rho_2^\beta\int_{z_{Gibbs}}^{\infty}\mathrm{d}z \quad (12)$$

where the position of the dividing surface between the solution and air phases, z_{Gibbs}, is chosen so that $\Gamma_1 = 0$, and ρ_2^α and ρ_2^β are, respectively, the (constant) densities of the solute in the bulk α (liquid, $z < z_{Gibbs}$) and β (gas, $z > z_{Gibbs}$) phases. Noting that, for an ion, $\rho_2^\beta = 0$, after rearranging eq 12, we obtain

$$\Gamma_2^1 = \int_{-\infty}^{z_{Gibbs}}[\rho_2(z) - \rho_2^\alpha]\,\mathrm{d}z + \int_{z_{Gibbs}}^{\infty}\rho_2(z)\,\mathrm{d}z \quad (13)$$

The first term is nonzero only when $\rho_2(z) \neq \rho_2^\alpha$, and it gives a negative contribution to Γ_2 when $\rho_2(z) < \rho_2^\alpha$ and a positive contribution when $\rho_2(z) > \rho_2^\alpha$. The second term gives a positive contribution to Γ_2 when $\rho_2(z) > 0$.

Figure 15 schematically depicts two classes of density profile, both based on simulation results for anions, which give $\Gamma_2 < 0$. Figure 15a shows the scenario embodied in the traditional view of salt solution/air interfaces, where the ions are repelled from the interface, as observed in simulations of F⁻. Figure 15b depicts the behavior observed in simulations of the heavier halide anions (e.g., Br⁻ and I⁻), where there is a density enhancement on the surface of the solution followed by a depletion in the subsurface region. For an oscillatory density profile, such as the one in Figure 15b, as long as the magnitude of the subsurface depletion is greater than the surface enhancement, the Gibbs surface excess will be negative. In this case, an increase of surface tension with salt concentration does not rule out the presence of ions at the interface. Thus, care should be taken when inferring interfacial composition from surface data on electrolyte solutions in cases where the ions exhibit oscillatory density profiles. Simulations with polarizable force fields predict that this is the case, e.g., for sodium bromide and iodide. Note, however, that in the simulations, which necessarily employ

a finite size of the unit cell, it is very difficult to obtain the subsurface ion depletion quantitatively. Indeed, while the surface peak of ions such as Br^- and I^- is well established in systems containing several hundreds of water molecules, the exact profile of the subsurface depletion is not completely converged and it is not presently known how large the system must be in order to fully quantitatively establish the surface–bulk equilibrium.[132]

Here we have restricted our attention to atomic anions which, according to simulations, can be either repelled from or adsorbed to the interface, depending on the ion. A similar analysis could be carried out for cations, but since inorganic cations are generally repelled from the interface, their behavior does not appear to contradict the conclusion drawn from a straightforward analysis based on the Gibbs adsorption equation. Note, however, that, for electroneutrality of the interfacial region, the Gibbs surface excesses of the anions and cations must be equal. For this reason, there is a subsurface sodium peak in the case of, e.g., NaBr or NaI solutions.[132]

Very recent simulations by Mucha et al.[135] suggest that the interfacial structure of solutions of strong acids and bases is essentially consistent with a standard application of the Gibbs adsorption equation to surface tension data. Within statistical uncertainty, the surface tension of the 1.2 M solution of HCl was the same as that of neat water and the surface tension of the HBr solution was lower than that of neat water by about 1 mN/m. The surface tension of the 1.2 M NaOH solution, however, was higher by about 4 mN/m. These results are semiquantitatively consistent with the experimental data plotted in Figure 14. A straightforward Gibbs adsorption analysis of the surface tension data predicts that the ions in acids adsorb to the interface, more so in HBr than in HCl, and that the ions in NaOH are repelled from the interface, which is precisely what is seen in the simulations (see Figure 11 and Figure 1 of ref 135).

4.2. Surface Potentials

According to eq 10, to have a nonzero surface tension, the tangential pressure must deviate from the normal (atmospheric) pressure in the interfacial region. Moreover, for a positive surface tension, the tangential pressure must be lower than the normal pressure. Water has a high surface tension, and this implies a large, negative tangential pressure, presumably reflecting substantial restructuring, and, more specifically, reorientation, of the water molecules to maximize their hydrogen bonding in the undercoordinated environment at the air/water interface. Thus, on average, the water molecules have a net orientation of their dipoles at the interface, in contrast to the isotropic orientation in the bulk liquid, and this contributes to a macroscopic electric potential difference across the liquid/air interface, $\chi = \varphi_{liquid} - \varphi_{air}$.

It has not been possible to directly measure the absolute value of the surface potential across the air/water interface. Given the fundamental importance of this quantity, there is a long list of estimates, both partially based on experimental measurements and purely theoretical, dating back to the 1920s.[167] The values derived from experimental data, mostly based on changes in the potential with electrolyte concentration, range from about -0.5 V to $+1.0$ V. Here, a positive value means that the liquid is positive relative to the vapor, and, assuming that the dipolar contribution is the most important, this implies that the water dipoles have a net orientation toward the liquid phase (i.e., H atoms pointing toward the liquid). Reviewers of the immense literature on the water surface potential have tended to favor positive values.[47,167,168]

Surface sensitive X-ray and nonlinear electronic and vibrational spectroscopies (discussed in more detail below) have provided some information on molecular orientation at the air/water interface, but the available information leads to potentially contradictory predictions of the sign of the surface potential. Second harmonic generation data for the air/water interface have been interpreted in terms of a net orientation of the dipole toward the bulk liquid,[169] which is consistent with a positive surface potential. On the other hand, vibrational sum frequency generation spectroscopy shows unambiguously that there is a substantial population of water molecules at the air/water interface with free (i.e., not hydrogen bonded) OH bonds,[52,170–172] and near-edge X-ray absorption fine-structure spectroscopy measurements on liquid microjets, in conjunction with density functional theory calculations, suggest that ~19% of the molecules on the water surface have both OH bonds free.[173] Since a majority of water molecules with free OH bonds are expected to have their dipoles tilted at least slightly toward the air side, these data would be consistent with a negative surface potential.

In principle, computer simulations could help at least to establish the sign of χ for the water/air interface. The results reported to date show a strong dependence on both the force field and the method of calculating the surface potential, and they span a wide range of values, although most simulations predict $\chi < 0$. Estimates by Matsumoto and Kataoka[174] and Barraclough et al.[168] based on integrating the density of molecular dipole moments have produced values of $+0.16$ V and $+0.24$ V, respectively, for water under ambient conditions, in apparent good agreement with the most commonly accepted experimentally derived values. However, when the potential is calculated more realistically by integrating the charge density, so that contributions from higher moments (most notably, the quadrupole moments) and finite molecular size are included,[175,176] it changes sign. For example, Wilson et al. obtained a value of $+0.79$ V by integrating the dipole density and -0.13 V by integrating the charge density from an MD simulation of the TIP4P water model.[176] Calculations based on the charge density have consistently produced negative surface potentials with magnitudes of a few hundred millivolts from simulations employing a variety of empirical force fields,[177] including the polarizable Dang–Chang potential,[149] and different electrostatic energy and force truncation schemes.[178] Ultimately, the discrepancy between the consensus experimental and simulation values may reside partially in the fact that the electrochemical techniques that are the basis of most of the experimental values contain a chemical contribution in addition to the electrostatic contribution that is computed from simulation trajectories.[175] It is also clear that computed surface potentials are sensitive to the details of the molecular charge distribution assumed in the force fields,[66,175,177] and so it is reasonable to suspect that inaccuracies in the force fields are an additional source of the discrepancy.

Changes of surface potential with composition of the solution can be measured and, when extrapolated to infinite dilution, afford $\Delta\chi = \chi(solution) - \chi(pure\ water)$,[47] which provides some insight into the changes of the structure of the air/water interface upon addition of solute. The values of $\Delta\chi$ are generally positive for alkali solutions of halide
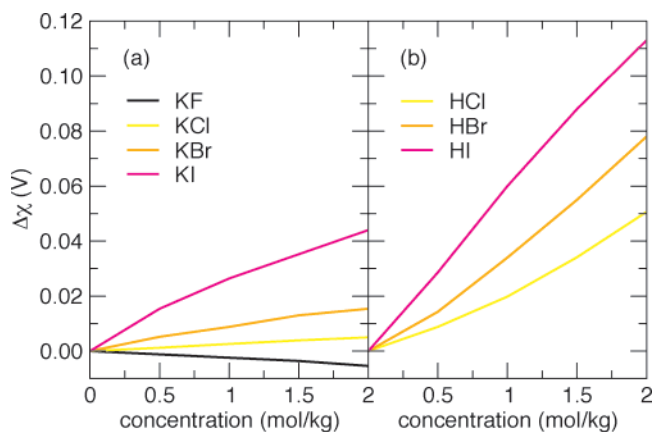
Figure 16. Changes in surface potential relative to pure water, $\Delta\chi = \chi(\text{solution}) - \chi(\text{pure water})$: (a) potassium halide salts; (b) corresponding strong acids (data from ref 47).

salts, e.g., KCl, KBr, and KI (Figure 16a), and this has been interpreted as being indicative of an ionic double layer near the surface with its negative side pointing toward the air and its positive side pointing toward the bulk solution; that is, the anions are closer to the interface than the cations.[47] The exception is KF, which exhibits a negative $\Delta\chi$, albeit with a relatively small magnitude which suggests that the anions and cations are well mixed in the interfacial region, with a slightly closer approach of the cation toward the surface. Our MD simulations of sodium halide solutions are entirely in accord with the interpretation of experimental $\Delta\chi$ values in terms of a double layer picture (see Figure 10). The anions approach the surface more closely than the cations in our simulations of NaCl, NaBr, and NaI, and the increase in anion adsorption in the order $Cl^- < Br^- < I^-$ is consistent with the order of the $\Delta\chi$ values at a given concentration, KCl < KBr < KI. Moreover, the slightly greater repulsion of F^- vs Na^+ from the interface in the simulation is consistent with the small, negative value of $\Delta\chi$ for KF.

The values of $\Delta\chi$ for the corresponding strong acids are also positive and increase in the order HCl < HBr < HI at a given concentration (Figure 16b).[47] The weak acid HF is anomalous due to incomplete dissociation and is therefore not discussed here.[47] Our simulation results (see Figure 10 of this review and Figures 1 and 2 of ref 135) are again consistent with the observed polarity and relative magnitudes of $\Delta\chi$ for these acids: the halide anions approach the surface more closely than the hydronium cations, and the adsorption of the ions increases in the expected order HCl < HBr < HI. Moreover, hydronium cations are oriented at the surface with their negatively charged oxygen atoms pointing into the gas phase.[116,135] The origin of the greater value of $\Delta\chi$ for the acid vs the corresponding salt (e.g., HI vs KI) at a given concentration, which is not obvious from the ion density profiles from the simulations, is a subject of ongoing research. The values of $\Delta\chi$ for KOH solutions are negative, with small magnitudes as in the case of KF.[47] Our simulation of NaOH predicts that Na^+ and OH^- are well mixed in the interfacial region,[135] and this is qualitatively consistent with the small magnitude of $\Delta\chi$ measured for KOH. Overall, it appears that MD simulations confirm the double layer picture that has been used to interpret experimental surface potentials for completely dissociated inorganic electrolytes (salts, acids, and bases).

4.3. Heterogeneous Chemical Processes

The recent resurgence of interest in the interfacial composition of electrolytes was to a large extent stimulated by experiments aimed at elucidating the role of heterogeneous processes in the chemistry of atmospheric aerosols. One of the first suggestions that heavier halide anions reside at the air/water interface, where they are available to react with gas-phase species, was made by Hu et al.[1] These authors studied the uptake of molecular halogens X_2 (X = Cl or Br) by droplets (with diameters of the order of 100 μm) of aqueous NaY (Y = Br^- or I^-) solutions, which was attributed primarily to the reaction $X_2 + Y^- \rightarrow XY + X^-$. The magnitude and concentration dependence of the measured uptake could not be described by a bulk phase reaction mechanism, and hence, Hu et al. suggested that reactions involving Y^- on the surfaces of the droplets play a significant role in the uptake process.[1]

Additional evidence for the presence of halide ions at the air/water interface has come from laboratory and kinetics modeling studies aimed at a developing a mechanistic description of the production of molecular halogens by sea salt particles that has been observed in field studies. Field measurements have detected the presence of Cl_2 in coastal air.[179] Br_2 and BrCl have been observed following polar sunrise in the Arctic,[7,180] presumably produced from halide precursors, e.g., sea salt deposited as aerosol particles on the snowpack. A chlorine atom precursor has been reported to be generated upon irradiation of seawater in the presence of ozone,[181] and the production of halogens in the Arctic has been correlated with depletion of ozone.[180]

Production of Cl_2 from both sea salt and NaCl aerosols via reaction with hydroxyl radical (generated by photolysis of ozone in the presence of water vapor) has been reproduced in laboratory aerosol chamber studies.[3,182] A chemical kinetics model based on 17 gas-phase species undergoing 52 reactions and 32 aqueous phase species undergoing 99 reactions underestimated the observed rate of Cl_2 production from NaCl aerosol by several orders of magnitude.[3] MD simulations performed in conjunction with this study predicted that the surface of a saturated NaCl solution contained a substantial population of chloride anions (occupying approximately 12% of the surface area), and they opened the door for consideration of a surface reaction. Quantum chemical calculations led to the proposal of a surface reaction proceeding via the formation of $OH\cdots Cl^-$ complexes which, when incorporated into the chemical kinetics model with reasonable estimates of unknown parameters, allowed us to reproduce the observed chlorine production semiquantitatively.[3] A subsequent MD simulation study of the uptake of OH by a concentrated NaCl solution showed that, while the presence of ions at the interface does not enhance the uptake, $OH\cdots Cl^-$ complexes do indeed form frequently, thus providing support for the proposed surface reaction.[183] Hydroxide anions, predicted to be a product in the proposed surface reaction, were recently detected in aqueous NaCl particles after exposure to OH.[4]

In addition to providing strong circumstantial evidence for the presence of chloride ions at the air/water interface, the combined experimental, theoretical, and kinetics modeling study summarized in the previous paragraph provided a mechanism for a potentially important source of highly reactive chlorine in the marine boundary layer. The consequences for air quality in a polluted region of chlorine production via the proposed surface reaction of OH and Cl^-

on the surface of sea salt particles were explored recently using an airshed model of the Los Angeles basin.[184] By comparing simulations with and without the surface reaction, it was demonstrated that chlorine emissions from sea salt could increase tropospheric ozone by as much as 12 ppb. Given that the air quality standard is set at 80 ppb for ozone, and the unavoidable background is generally around 40 ppb, the contribution from the interfacial chlorine chemistry is appreciable.

An interfacial reaction has also been implicated in the production of Br_2 via oxidation of bromide anions by ozone in sea salt in another comprehensive investigation involving aerosol chamber kinetics measurements, MD simulations, and computational kinetics modeling.[185] Similar to the case of the OH reaction with NaCl particles, the measured rate of Br_2 production by deliquesced NaBr particles upon exposure to ozone (in the absence of ultraviolet radiation) in the aerosol chamber was underpredicted (by roughly an order of magnitude) by the kinetics model, which included all known bulk aqueous and gas-phase chemistry. Consistent with our previous study,[132] the MD simulations predicted a substantial population of bromide anions on the surface of 1.2 M and ~6 M NaBr solutions. Moreover, MD simulations of the ozone uptake by the NaBr solutions revealed that the ozone accumulates on the surface, where it has a long residence time, and O_3-Br^- contacts are frequent and last up to 50 ps. A novel interfacial reaction for the production of Br_2 from Br^- via the formation of O_3-Br^- complexes was, therefore, incorporated into the computer kinetics model, and good agreement with the aerosol chamber data was obtained. Extrapolation of the results of this study to atmospheric conditions suggested that the contribution of the surface reaction should be at least competitive with the bulk aqueous phase chemistry.

Seawater contains a relatively low concentration of bromide anions (the chloride-to-bromide ratio is roughly 650). The relevance in the atmosphere of the chemistry studied in the aerosol chamber experiments, which were performed using particles with bromide concentrations roughly a factor of 1000 higher than that of seawater, was established by additional considerations.[185] Key among these is the finding that bromide anions selectively adsorb to the surface of concentrated solutions of chloride salts containing a small amount of bromide anions. This selective enhancement of bromide at the interface has been observed in both MD simulations and experiments that will be discussed in the next subsection.

4.4. Photoelectron Spectroscopy

The experiments discussed thus far in this section have been used to infer the interfacial composition of electrolyte solutions either from macroscopic properties of the surface as a whole (e.g., surface tension or surface potential) or by using circumstantial evidence from presumed heterogeneous chemical reactions. Roughly a decade ago, surface sensitive techniques that probe particular chemical species began to be applied to aqueous salt solutions. One of these is photoelectron spectroscopy, which involves analysis of the kinetic energies of electrons ejected from materials following impact by photons. The species selectivity comes from the ability to derive electron binding energies (valence or core) from the photoelectron kinetic energies, and the surface selectivity comes from the limited mean free path of electrons in condensed matter. Photoelectron signals from ions and

water molecules have been used in several studies to elucidate the surface compositions of aqueous salt solutions.

Böhm et al. measured He(I) photoelectron spectra from the surfaces of highly concentrated aqueous CsF solutions ($CsF\cdot4.2H_2O$ to $CsF\cdot2.6\ H_2O$).[186] Using absolute photoionization cross sections, they were able to relate the signal strengths of the ions to those of the water molecules, and the results suggested that the ions were strongly depleted in the interfacial region. Furthermore, they estimated that the salt free zone was roughly two water monolayers thick. The depletion of CsF from the interface is consistent with MD simulation results for NaF (Figure 10) and the traditional view of an ion-free interface inferred from surface tension data for salts composed of hard ions (Figure 15a). Addition of a small amount of CsI to a solution of $CsF\cdot3H_2O$ produced a significant change in the photoelectron signal that led Böhm et al. to conclude that I^- was surface active. Although in such a highly concentrated solution it is not clear that the surface activity is intrinsic and not a consequence of crowding out, this appears to be the first suggestion of the surface activity of a halogen anion.

The surface activity of the heavier halogen anions was the subject of several recent photoelectron spectroscopic studies. Weber et al. reported valence band photoemission data on liquid microjets of alkali metal iodide solutions spanning a wide range of concentration ($0.5-12\ m$).[57] Their data were were consistent with a negative surface excess for NaI and showed essentially no cation selectivity. The absence of anion enhancement on the surface appears to contradict the predictions of MD simulations, but the probe depth of the experiments, purported to be a few water layers, was insufficient for resolving the relatively small scale inhomogeneities in the ion density profiles observed in the simulation results (Figure 10). Analogous experiments performed on tetrabutylammonium iodide (TBAI) solutions showed a large enhancement of iodide at the interface in TBAI(aq) vs NaI-(aq), which was backed up by MD simulations.[58] Evidently, the strongly surface active hydrophobic TBA cations drag additional iodide anions to the surface in order to maintain local electroneutrality.

The surface composition of concentrated solutions of KBr and KI (specifically, freshly cleaved crystals exposed to water vapor up to the deliquescence point) has very recently been probed with high spatial resolution using high-pressure X-ray photoelectron spectroscopy.[187] The anion/cation ratios were determined as a function of photoelectron energy, which, because of the energy dependence of the electron mean free path, is a measure of the probe depth. The data demonstrated that the anion concentrations were enhanced relative to the cation concentrations in the interfacial region, more so for iodide than bromide (Figure 17). Thus, the results appeared to validate the qualitative predictions of MD simulations.[132] As a matter of fact, the experimental data indicated that the anion enhancement at the interface is even greater than that observed in the simulations.

To gain insight into the relatively high reactivity of bromide toward ozone despite its low abundance compared to chloride in sea salt aerosols, X-ray photoelectron measurements were performed on bromide-doped NaCl crystals.[59] On the dry surface the ratio of bromide to chloride was found to be the same as that in the bulk crystal. However, following exposure to water vapor and redrying, the bromide to chloride surface ratio increased significantly, and scanning electron microscopy images revealed that NaBr crystallites form on
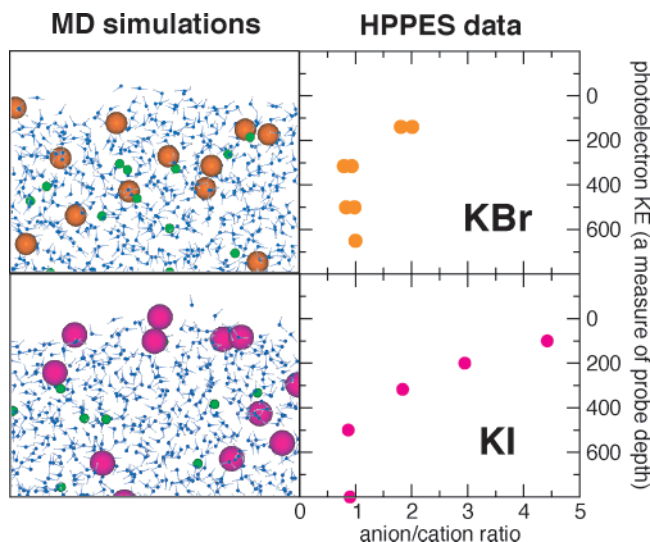
Figure 17. Left panels: snapshots from MD simulations of 1.2 M NaBr and NaI solutions (data from ref 132). Right panels: anion/cation ratios in concentrated KBr and KI solutions determined by high-pressure X-ray photoelectron spectroscopy as a function of photoelectron kinetic energy, i.e., probe depth (data from ref 187).

Figure 18. Vibrational sum frequency generation spectra in the region of the water OH stretching frequency for neat water and NaI solutions: (a) experimental spectra;[53] (b) spectra computed from MD trajectories,[199] normalized to have the same intensity at 3700 cm^{-1}. MD results are shown for 1.2 M NaI solutions in which the ions were modeled with a polarizable force field, which gave a strong anion adsorption, and a nonpolarizable force field, which gave a moderate anion adsorption.

the surface. Thus, with sufficient water present to provide ionic mobility, bromide appears to segregate to the surface of a salt solution containing both bromide and chloride. This phenomenon was subsequently confirmed by MD simulations.[69] A single bromide anion placed on the surface of a slab of a ~6 M NaCl solution remained there during the entire 800 ps simulation, while in a second simulation a single bromide anion placed initially in the middle of the slab found its way to the surface after 300 ps and remained there for the rest of the trajectory. The concentration dependence of the relative surface propensities of bromide and chloride was explored in additional simulations. In a low-concentration mixture of NaBr and NaCl (each at 0.6 M), the interfacial concentration of bromide was enhanced relative to that of chloride by a factor roughly equal to the ratio of interfacial concentrations found in pure solutions of 1.2 M NaBr and 1.2 M NaCl. However, in a higher concentration mixture (3.0 M each), the bromide anions were selectively enhanced at the expense of chloride anions, which were displaced by bromide from the interfacial region. Thus, both photoelectron spectroscopy and MD simulations support the notion that the enhanced reactivity of bromide in sea salt is at least in part due to surface segregation of the bromide anions.

4.5. Surface Selective Nonlinear Spectroscopies

Second harmonic generation and vibrational sum frequency generation are nonlinear optical processes that probe the second-order nonlinear susceptibility of the medium. In the case of SHG, the incident beam is at a frequency ω, typically in the visible region of the spectrum, and the output is at 2ω, while for VSFG the incident frequencies, ω_{IR} and ω_V, are typically in the infrared and visible, respectively, and the output is at $\omega^{SFG} = \omega_{IR} + \omega_V$. When the frequency of the incident radiation (ω in the case of SHG and ω_{IR} in the case of VSFG) is coincident with a transition in the medium (electronic for SHG and vibrational for VSFG), the output signal is resonantly enhanced. As second-order processes, within the dipole approximation, both SHG and VSFG are forbidden in media with inversion symmetry (e.g.,
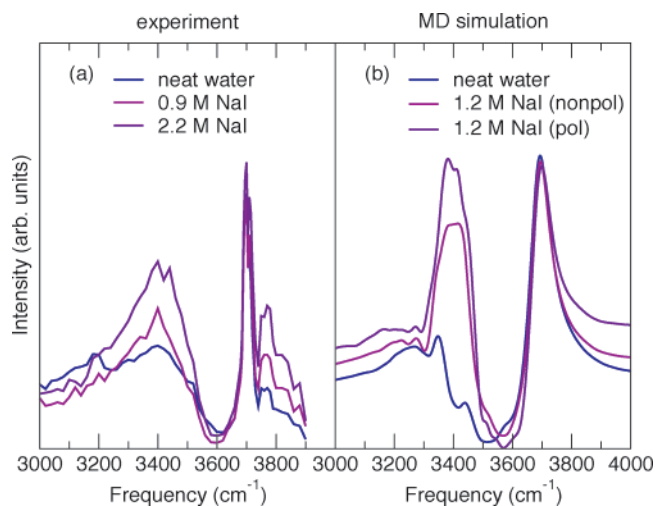
bulk solutions) but are allowed where inversion symmetry is broken (e.g., at surfaces and interfaces). For recent reviews of the techniques and applications of SHG and VSFG spectroscopies to aqueous interfaces, see refs 171, and 188–190 and several reviews in this special issue. Here, we briefly review recent VSFG studies that indirectly probe the surface composition of aqueous electrolyte solutions through observation of changes in the vibrational spectrum of water molecules in the interfacial region, and SHG studies that directly probe electronic transitions of ions at the air/solution interface.

VSFG spectra of aqueous systems are usually measured over a spectral range spanning water OH stretching frequencies. The water OH stretching frequency is sensitive to the hydrogen bonding environment and, hence, reports indirectly the presence of solutes in the interfacial region via their interactions with water molecules. A typical VSFG spectrum measured for the neat air/water interface using the ssp polarization combination is shown in Figure 18a. Although other polarization combinations are possible,[191] the ssp combination, which probes transition dipoles perpendicular to the interface, is the most commonly employed. The ssp polarized VSFG spectrum of the air/water interface displays two prominent features: a sharp peak at ~3700 cm^{-1} and a broad band spanning ~3100 cm^{-1} to ~3600 cm^{-1}. Within the latter there appears to be two peaks, one centered around 3200 cm^{-1} and the other around 3400 cm^{-1}.

The ability to infer structure and intermolecular interactions from VSFG spectra relies heavily on the assignment of the spectral features. The assignments of vibrational spectra of interfacial water, which are based on assignments of linear-IR and Raman spectra of ice, water, and aqueous solutions, have been discussed extensively elsewhere,[52,171,192,193] so we give just a brief summary here. The peak at 3700 cm^{-1} is generally attributed to uncoupled "free" OH oscillators not participating in hydrogen bonding interactions. It is reasonable to expect that the majority of the free OH bonds are protruding from the surface of the liquid. The lower frequency bands are definitely attributable to OH oscillators

involved in hydrogen bonding, but the precise origin of the bands is a subject of ongoing discussion, and it is safe to say that, at this time, their assignment remains controversial. Broadly speaking, there are two schools of thought. One attributes the 3400 cm^{-1} feature to disordered but hydrogen bonded water molecules on the surface, e.g., the hydrogen bonded OH bond ("donor" OH) of a water molecule containing a free OH bond, and the 3200 cm^{-1} band to OH bonds in tetrahedrally coordinated water molecules. The other posits that the donor OH participates in strong hydrogen bonds and, hence, is the origin of the 3200 cm^{-1} band, while the tetrahedrally coordinated water molecules give rise to the 3400 cm^{-1} band. A very recent theoretical analysis also suggests that the 3400 cm^{-1} band is due to tetrahedrally coordinated water molecules, while the 3200 cm^{-1} band arises from collective excitations of intermolecularly coupled vibrations.[194]

There have been several reports of theoretical calculations of the VSFG spectrum from MD simulations of the air/water interface. The first was from Benjamin,[195] who actually computed an IR spectrum for molecules in the interfacial region and compared it to the corresponding bulk IR spectrum. The surface IR spectrum qualitatively resembled the experimental VSFG spectrum, and the simulation confirmed that the sharp, high-frequency band was due to a high population (~25%) of free OH bonds on the surface of the liquid. A surface IR spectrum computed from an ab initio MD simulation of the air/water interface exhibited similar, qualitative agreement with experimental VSFG spectra.[196]

Three different approaches to computing the more complicated (compared to the case of surface IR) VSFG line shape from MD simulations of water have been developed by two groups. Morita and Hynes developed two approaches. The first is applicable to configurations sampled from MD simulations of rigid water models and incorporates environmental effects on the normal modes of the OH stretching vibrations, their frequency shifts, and hyperpolarizability but treats the nonresonant contribution as an adjustable parameter.[192] The second is a time dependent approach in which the resonant contribution (frequency dependent hyperpolarizability) is expressed in terms of the time correlation function of the system polarizability tensor and dipole moment, which is computed from an MD simulation of a flexible water model, including electronic polarization effects.[197] Both approaches predicted VSFG spectra for the air/water interface that were in good qualitative agreement with experimental spectra. Analysis of the nonlinear susceptibilities revealed that the high-frequency band of the VSFG spectrum is essentially determined by the free OH oscillators in the topmost layer of the liquid, while the broad, low-frequency band contains contributions from subsurface water molecules. Perry et al.[198] developed a method for computing the VSFG spectrum from instantaneous normal modes (INM), as well as a time correlation function (TCF) approach similar to that of Morita and Hynes.[197] Both the TCF and INM spectra computed by Perry et al. from MD simulations of a flexible water model were qualitatively similar to experimental results. The INM method enables the spectrum to be decomposed into contributions from individual modes, and Perry et al. used this feature to show that antisymmetric stretching dominates the spectrum at higher frequencies, while symmetric stretching dominates at lower frequencies, and that OH stretches on the surface of the liquid are primarily local modes.

The strength of the VSFG response for a given polarization combination depends on several factors,[52,197] including the oscillator strengths and phases of the vibrations being probed, the number of oscillators contributing from a noncentrosymmetric environment (i.e., the width of the inhomogeneous region in liquid/air interfacial systems), the degree of orientational ordering of the oscillators, and local field effects. All of these factors must be considered, in addition to having at hand an assignment of spectral features at some level, when inferring changes in composition and intermolecular interactions in the interfacial region upon addition of solutes to water. In some cases the changes in the spectra are dramatic, and hence, a qualitative molecular level description of the perturbation of the interfacial structure is straightforward, while in other cases the changes are subtle, leaving room for ambiguities in the interpretation.

An example of the latter is the case of the sodium halide solutions. Essentially the same sets of VSFG spectra of ~1 to ~2 M aqueous solutions of NaF, NaCl, NaBr, and NaI were reported by two independent groups at roughly the same time recently.[53,54] The spectra of the NaF and NaCl solutions were found to be very similar to the neat water spectrum (similar results for NaCl were reported previously by Schnitzer et al.[50]), while the spectra for NaBr and NaI exhibited an enhancement of intensity in the 3400 cm^{-1} band that grew with increasing salt concentration (for example, see the NaI data from Liu et al.[53] shown in Figure 18). Both reports discussed the spectra in terms of our MD simulations,[132] which predicted that the heavier halide anions adsorb to the air/water interface. On the basis of the comparison of the VSFG spectra with bulk IR and Raman data, Liu et al.[53] concluded that there was a higher concentration of bromide and iodide anions in the interfacial region with a concomitant increase in interfacial depth, consistent with the predictions of the MD simulations. Meanwhile, Raymond and Richmond,[54] on the basis of spectral fitting with assignments based on isotopic dilution measurements, concluded that, while there are anions in the interfacial region probed by the experiments (signaled by changes in bands assigned to tetrahedrally coordinated water), the insensitivity of the donor OH band to addition of salt indicates a significantly diminished population of anions in the uppermost layer of the solutions. The latter contradicts the predictions of the MD simulations. The somewhat different conclusions reached by two groups interpreting essentially the same data indicate that more work is required to unambiguously assign the features in the hydrogen bonded OH region of the VSFG spectrum of aqueous solutions.

A very recent MD simulation study suggests that the increase of the band at 3400 cm^{-1} upon addition of the heavier halides is correlated with the population of anions at the air/solution interface.[199] Brown et al. applied the Morita−Hynes TCF approach to compute the VSFG spectra of neat water and 1 M sodium iodide solutions.[199] The flexible, nonpolarizable model of water developed by Ferguson[200] was used for water, and two separate simulations of aqueous sodium iodide employed either polarizable or nonpolarizable models for the ions. Both models led to an adsorption of iodide anions to the interface, but it was much less pronounced in the nonpolarizable model vs the polarizable one. The resulting VSFG spectra are shown in Figure 18b. Consistent with the experimental spectra (Figure 18a), there is an increase in the 3400 cm^{-1} band upon addition of NaI. The increase (vs the case of neat water) relative to the

free OH band is larger for the polarizable iodide compared to the nonpolarizable iodide, and this reinforces the correlation between the increase in the intensity of the 3400 cm^{-1} band and the adsorption of the anions to the solution/air interface.

In contrast to the case of the sodium halide salts, addition of the corresponding acids (HX; X = Cl$^-$, Br$^-$, I$^-$) to water gives rise to pronounced changes throughout the OH stretching region of the VSFG spectrum. Spectra measured in different laboratories all show a decrease in the intensity of the free OH band and an increase in intensity throughout the range of hydrogen bonded bands in the acid solutions vs neat water.[50,135] In a very recent combined VSFG and MD simulation study of salt, acid, and base solutions,[135] it was found that the perturbation of the VSFG spectrum of HX solutions vs neat water increased in the order HCl < HBr < HI. Moreover, in the same study, additional intensity below 3200 cm^{-1} in spectra of HX solutions, which was not seen for neat water or aqueous NaCl and NaOH, was attributed to Eigen[109] (hydronium) and Zundel[110] cations. The VSFG spectrum of aqueous NaOH was essentially identical to the spectrum of NaCl, which was in turn very similar to the neat water spectrum. The qualitative trends in the VSFG spectra appeared to confirm the predictions of the MD simulations, namely, that in acid solutions the hydronium cation is a surface active species along with the heavier halide anions, while the sodium cation and hydroxide anion are repelled from the interface. The agreement between the VSFG and MD results was strengthened by free OH bond populations computed from the simulations, which tracked the intensity of the free OH peaks in the VSFG spectra.

Another very recent combination of VSFG spectroscopy and MD simulations sought to characterize the interfaces of aqueous solutions containing the important atmospheric aerosol species, ammonium and sulfate ions.[144] The simulations of sulfate solutions at finite concentration reinforced predictions from an earlier simulation at infinite dilution that sulfate anions are strongly repelled from the air/water interface.[103] An interesting consequence is that the positively charged counterions approach the interface more closely than the anions; this is true slightly more so for ammonium than for sodium. This results in an electrical double layer at the interface that has the opposite polarity of that in halide solutions, e.g., the ammonium chloride considered in the present study,[144] and the sodium halides (NaCl, NaBr, and NaI) studied previously.[132] The predictions of the simulations were backed up by surface tension measurements and the VSFG spectra. Pronounced differences between the spectra of neat water, ammonium chloride, sodium sulfate, and ammonium sulfate were observed, primarily in the hydrogen bonded OH region of the spectrum: ammonium chloride produced a small increase of intensity around 3400 cm^{-1}, while the sulfate salts increased the intensity throughout the hydrogen bonded region, more so with the ammonium than with the sodium counterion. The spectral changes were considered in light of a detailed analysis of the MD simulations, and could be explained primarily in terms of differences in the interfacial widths, specifically, a broadening of the interface of the electrolyte solutions vs neat water that is greatest for the sulfate solutions, but not in terms of changes in the populations of free and hydrogen-bonded OH bonds.

SHG measurements based on charge-transfer-to-solvent (CTTS) transitions in inorganic anions have recently been applied by Saykally and co-workers to the quantification of the adsorption of several ions to the air/water interface.[55,56,147,201] In each case, the concentration dependence of the SHG response of the anion was found to be described well by a Langmuir isotherm, from which surface excess free energies could be estimated. The free energy values for the azide and iodide anions were found to be −2.4 kJ/mol and −6.2 kcal/mol, respectively.[55,56] Thus, the SHG data indicate that both of these anions adsorb strongly to the air/water interface. In the case of the iodide anion, the surface population appeared to saturate at a bulk concentration of about 100 mM. The strong surface propensity of iodide revealed by the SHG data is qualitatively consistent with the results of MD simulations,[132,133] but the experimentally derived free energy of adsorption is considerable larger than that estimated either by direct free energy calculations or from the ratio of surface to bulk concentrations in the simulations. The increase in iodide adsorption detected by SHG in HI vs NaI or KI was recently used to argue that the hydronium cation adsorbs to a greater extent than the alkali metal cations,[201] and this provides additional support to the surface activity of hydronium cations in hydrogen halide acids predicted by MD simulations.[135] SHG and MD simulations also corroborated each other in a very recent collaborative investigation of the surface activity of the thiocyanate anion.[147] The SHG data exhibited an onset of saturation in the surface concentration of the anion at a bulk concentration of about 1 M, which was consistent with the trend in interfacial anion populations observed in the simulations. This study, along with others summarized in this subsection, illustrates the utility of combining state-of-the-art surface sensitive spectroscopic measurements with MD simulations in order to elucidate the interfacial structure of aqueous electrolyte solutions. Ongoing collaborative efforts along these lines will continue to provide additional insight into the microscopic details of structure and dynamics at aqueous interfaces in the near future.

5. Future Developments

Recent significant progress in computations, theory, and experiments concerning specific ion effects at the air/water interface is changing our perception of surfaces of electrolytes and, at the same time, raising new questions. The first class of questions concerns future developments in computational techniques. Most of the computational results presented in this review are based on molecular dynamics simulations employing relatively simple polarizable potentials. New, more sophisticated and accurate force fields[152−156] are now becoming available and are starting to be used in this type of simulations. This force field development, in combination with the use of larger system (unit cell) sizes and longer simulations, should provide more quantitative and converged results and also allow studying hitherto unexplored molecular ions, for which interaction potentials have not been constructed yet. Although it is unlikely that such simulations will significantly change the present picture, it is desirable to eventually reach the limits of the predictive power of classical MD simulations.

At the same time, thanks to continuous progress in hardware and software, ab initio molecular dynamics simulations for relevant system sizes (hundreds to thousands of atoms) and time scales (hundreds of picoseconds to nanoseconds) will become feasible in the near future. On one hand, the prospect of exploring propensities of ions for extended aqueous interfaces with electronic structure and

forces evaluated from first principles is exciting. This has been the obvious "next step" for quite a while, hindered only by immense requirements on computational resources. On the other hand, it remains to be established whether the present standard level of electronic structure theory in ab initio molecular dynamics (i.e., the BLYP or similar density functionals) is sufficient for quantitative predictions or whether it will be necessary to employ more accurate (and costly) quantum chemical approaches.

The future will hopefully also bring progress in theories of surfaces of aqueous electrolytes. It is always desirable to have a simple, elegant, and correct model which allows performing fast back-of-the-envelope calculations (rather than tedious and time-consuming simulations) to provide at least semiquantitative estimates. At present, several continuum models exist, which respect ions specificity by including dispersion, polarization, and solvophobic forces.[23,31−33,35,36,65] There has clearly been tremendous progress since the early model by Onsager and Samaras.[22] Nevertheless, the present theories still suffer from several shortcomings. The first one, the neglect of the detailed molecular structure of at least the first solvation shell around the ion, is inherent to continuum models. Possibly, some kind of a shell model, which would respect the "granularity" of the solvent at short separations, could be applied to the study of ions at aqueous interfaces in the near future. The second shortcoming of some of the present continuum theories is that they to a certain extent involve ad hoc assumptions, e.g., concerning adsorption of specific ions at the aqueous surface.[32] The future will probably bring refined theories which will "connect hierarchies" in the sense that they will respect converged results at the molecular level. These can be provided primarily by electronic structure calculations and ab initio molecular dynamics, which give a picture with atomic resolution, albeit mainly for small systems.

The progress in surface selective experimental techniques for probing the air/solution interface has been spectacular in the last half decade. A major leap forward has been achieved by minimizing the system size (e.g., via microjets), allowing for the application of standard vacuum techniques for volatile liquids such as water. Another way to circumvent the vapor problem is to use amorphous solid water as a model for liquid water. An important issue for methods such as the high-pressure photoelectron spectroscopy or nonlinear vibrational and optical techniques is to quantitatively establish the probing depth. This is highly nontrivial for a (sub)-nanometer liquid interface, which exhibits disorder, corrugation, and capillary waves. Nevertheless, there is good hope that in the near future our experimental knowledge of aqueous interfaces will approach in accuracy and detail that of solid-state surfaces.

6. Conclusions

A new view of inorganic ions at the air/water interface is emerging from recent simulations and surface selective spectroscopic experiments. Traditionally, surfaces of aqueous electrolytes are described as inactive and practically devoid of ions.[22,47] This turns out to hold for hard (nonpolarizable) ions, such as fluoride and alkali cations. Multiply charged ions, such as sulfate, are also strongly repelled from the surface, but due to strong electrostatic interaction, they tend to structure and broaden the interfacial water layer.[144] However, due to specific ion effects, and polarization interactions in particular, soft (polarizable) monovalent anions, such as the heavier halides and other polarizable inorganic anions, exhibit a propensity for the air/water interface.[69,132,134,203] Similarly, the hydronium cation shows an affinity for the aqueous surface, albeit primarily due to its specific hydrogen bonding features.[113,116,135]

Calculations show the importance of a detailed molecular description of the air/solution interface which accounts both for interactions within the first solvation shell and for long-range effects. In particular, ion and water polarization, solvent exclusion, and hydrogen bonding rearrangements determine whether a particular ion is found at the aqueous surface. The "virtual reality" of molecular dynamics simulations is internally consistent in the sense that the use of a broad range of polarizable force fields results in the surface activity of soft anions and hydronium cations.[69,116,132,135,158] These force fields also benchmark well against ab initio results for the structures of ion-containing water clusters.[92−94,97,98,114]

More importantly, predictions from MD simulations are supported by mounting experimental evidence for the presence of ions such as heavier halides, azide, thiocyanate, and hydronium at aqueous surfaces. Unlike solid-state surfaces, the air/water interface is hard to probe experimentally. This (sub)nanometer layer is corrugated, disordered, and nonstationary, being subject to capillary waves. Nevertheless, new experimental surface selective techniques applied to electrolyte solutions, such as high-pressure photoelectron spectroscopy (PES)[57,187] or electronic (SHG)[55,56,201] and vibrational[53] (VSFG) nonlinear spectroscopies, together with scanning electron miscroscopy (SEM),[59] ion sputtering,[60,61] and metastable impact electron spectroscopy (MIES)[62] directly or indirectly point to the presence of heavier halides and other soft anions, as well as that of hydronium at the air/water interface. Arguably, it is still too early to claim that the occurrence of these ions at aqueous surfaces is established beyond reasonable doubt; however, the body of computational and experimental evidence is significant and steadily increasing.

The presence of inorganic ions at aqueous interfaces has important consequences for heterogeneous physics and chemistry relevant both for technology and for atmospheric processes. This is true for extended aqueous surfaces and, in particular, for small droplets which have a large surface-to-bulk ratio. Probably the best known example of such a process is the production of molecular chlorine and other reactive halogen compounds at the surfaces of aqueous sea salt aerosols in the polluted marine boundary layer and in atmospheric chambers mimicking the tropospheric conditions.[1−5,182] Another atmospherically relevant case is the destruction of tropospheric ozone in high-latitude regions by reactive bromine species (Br_2 and $BrCl$). It is now well established that these halogen compounds are released by chemical reactions from the bromide enriched surface of the sea spray covered Arctic snowpack during polar sunrise.[7,69,180] In summary, halide ions at aqueous surfaces contribute to the production of halogens in the lower atmosphere. This influences oxidative processes and thus affects both chemistry and physics (such as droplet growth and, consequently, e.g., climatic effects of aerosols) in the troposphere.

While the consequences of the presence of inorganic anions, such as the heavier halides and others, at aqueous surfaces have been broadly discussed, we are only now starting to realize the possible implications of the propensity of hydronium for surfaces of acid solutions. For example, it is well established that adding an alkali halide salt to water

inhibits bubble coalescence (which is one of the reasons why wave activity creates foam on the ocean but not on freshwater lakes), while adding the corresponding acid has no effect.[8,9,11,12] Possibly, the much weaker surface segregation of cations and anions in these acids compared to the salts is responsible for this behavior. The presence of hydronium cations at aqueous surfaces should also have consequences for chemistry, such as corrosion processes, both in the atmosphere and in technological applications. It is likely that many more hitherto unexplored effects will be discovered now that the surface propensity of hydronium cations and soft (polarizable) inorganic anions has been established.

7. References

(1) Hu, J. H.; Shi, Q.; Davidovits, P.; Worsnop, D. R.; Zahniser, M. S.; Kolb, C. E. *J. Phys. Chem.* **1995**, *99*, 8768.
(2) Finlayson-Pitts, B. J.; Hemminger, J. C. *J. Phys. Chem. A* **2000**, *104*, 11463.
(3) Knipping, E. M.; Lakin, M. J.; Foster, K. L.; Jungwirth, P.; Tobias, D. J.; Gerber, R. B.; Dabdub, D.; Finlayson-Pitts, B. J. *Science* **2000**, *288*, 301.
(4) Laskin, A.; Gaspar, D. J.; Wang, W. H.; Hunt, S. W.; Cowin, J. P.; Colson, S. D.; Finlayson-Pitts, B. J. *Science* **2003**, *301*, 340.
(5) Finlayson-Pitts, B. J. *Chem. Rev.* **2003**, *103*, 4801.
(6) Oum, K. W.; Lakin, M. J.; Finlayson-Pitts, B. J. *Geophys. Res. Lett.* **1998**, *25*, 3923.
(7) Spicer, C. W.; Plastridge, R. A.; Foster, K. L.; Finlayson-Pitts, B. J.; Bottenheim, J. W.; Grannas, A. M.; Shepson, P. B. *Atmos. Environ.* **2002**, *36*, 2721.
(8) Craig, V. S. J.; Ninham, B. W.; Pashley, R. M. *Nature* **1993**, *364*, 317.
(9) Craig, V. S. J.; Ninham, B. W.; Pashley, R. M. *J. Phys. Chem.* **1993**, *97*, 10192.
(10) Weissenborn, P. K.; Pugh, R. J. *Langmuir* **1995**, *11*, 1422.
(11) Marcelja, S. *Curr. Opin. Colloid Interface Sci.* **2004**, *9*, 165.
(12) Craig, V. S. J. *Curr. Opin. Colloid Interface Sci.* **2004**, *9*, 178.
(13) Shcherbina, A. Y.; Talley, L. D.; Rudnick, D. L. *Science* **2003**, *302*, 1952.
(14) Kritzer, P. *J. Supercrit. Fluids* **2004**, *29*, 1.
(15) Tucceri, R. *Surf. Sci. Rep.* **2004**, *56*, 85.
(16) Tavares, F. W.; Bratko, D.; Prausnitz, J. M. *Curr. Opin. Colloid Interface Sci.* **2004**, *9*, 81.
(17) Gradzielski, M. *Curr. Opin. Colloid Interface Sci.* **2004**, *9*, 256.
(18) Cacace, M. G.; Landau, E. M.; Ramsden, J. J. *Q. Rev. Biophys.* **1997**, *30*, 241.
(19) Piazza, R. *J. Cryst. Growth* **1999**, *196*, 415.
(20) Born, M. *Z. Phys.* **1920**, *1*, 45.
(21) Wagner, C. *Phys. Z.* **1924**, *25*, 474.
(22) Onsager, L.; Samaras, N. N. T. *J. Chem. Phys.* **1934**, *2*, 528.
(23) Markin, V. S.; Volkov, A. G. *J. Phys. Chem. B* **2002**, *106*, 11810.
(24) Kharkats, Y. I.; Ulstrup, J. *J. Electroanal. Chem.* **1991**, *308*, 17.
(25) Stern, F. *Phys. Rev. B* **1978**, *17*, 5009.
(26) Rahman, T. S.; Maradudin, A. A. *Phys. Rev. B* **1980**, *21*, 504.
(27) Palasantzas, G. *J. Appl. Phys.* **1997**, *82*, 351.
(28) Yu, K. W.; Sun, H.; Wan, J. T. K. *Physica B* **2000**, *279*, 78.
(29) Lynden-Bell, R. M.; Rasaiah, J. C. *J. Chem. Phys.* **1997**, *107*, 1981.
(30) Lynden-Bell, R. M.; Rasaiah, J. C.; Noworyta, J. P. *Pure Appl. Chem.* **2001**, *73*, 1721.
(31) Manciu, M.; Ruckenstein, E. *Adv. Colloid Interface Sci.* **2003**, *105*, 63.
(32) Karraker, K. A.; Radke, C. J. *Adv. Colloid Interface Sci.* **2002**, *96*, 231.
(33) Frediani, L.; Mennucci, B.; Cammi, R. *J. Phys. Chem. B* **2004**, *108*, 13796.
(34) Kunz, W.; Lo Nostro, P.; Ninham, B. W. *Curr. Opin. Colloid Interface Sci.* **2004**, *9*, VII.
(35) Levin, Y. *Pramana* **2005**, *64*, 957.
(36) Kunz, W.; Belloni, L.; Bernard, O.; Ninham, B. W. *J. Phys. Chem. B* **2004**, *108*, 2398.
(37) Allen, M. P.; Tildesley, D. J. *Computer Simulations of Liqiuds*; Clarendon: Oxford, 1987.
(38) Laasonen, K.; Sprik, M.; Parrinello, M.; Car, R. *J. Chem. Phys.* **1993**, *99*, 9080.
(39) Koch, W.; Holthausen, M. C. *A Chemist's Guide to Density Functional Theory*; Wiley-VCH: Weinheim, 2000.
(40) Heydweiller, A. *Ann. Phys.* **1910**, *33*, 145.
(41) Gibbs, J. W. *The Collected Works of J. Willard Gibbs*; Longmans: New York, 1928.
(42) Debye, P. W.; Huckel, E. *Phys. Z.* **1923**, *24*, 185.
(43) *International Critical Tables*; Washburn, E. W., Ed.; McGraw-Hill: New York, 1928; Vol. 4.
(44) Weissenborn, P. K.; Pugh, R. J. *J. Colloid Interface Sci.* **1996**, *184*, 550.
(45) Adam, N. K. *The Physics and Chemistry of Surfaces*; Oxford University Press: London, 1941.
(46) Randles, J. E. B. *Faraday Soc. Discuss.* **1957**, *24*, 194.
(47) Randles, J. E. B. *Phys. Chem. Liq.* **1977**, *7*, 107.
(48) Hofmeister, F. *Arch. Exp. Pathol. Pharmakol. (Leipzig)* **1888**, *24*, 247.
(49) Baldelli, S.; Schnitzer, C.; Shultz, M. J. *Chem. Phys. Lett.* **1999**, *302*, 157.
(50) Schnitzer, C.; Baldelli, S.; Shultz, M. J. *J. Phys. Chem. B* **2000**, *104*, 585.
(51) Shultz, M. J.; Schnitzer, C.; Simonelli, D.; Baldelli, S. *Int. Rev. Phys. Chem.* **2000**, *19*, 123.
(52) Shultz, M. J.; Baldelli, S.; Schnitzer, C.; Simonelli, D. *J. Phys. Chem. B* **2002**, *106*, 5313.
(53) Liu, D. F.; Ma, G.; Levering, L. M.; Allen, H. C. *J. Phys. Chem. B* **2004**, *108*, 2252.
(54) Raymond, E. A.; Richmond, G. L. *J. Phys. Chem. B* **2004**, *108*, 5051.
(55) Petersen, P. B.; Saykally, R. J. *Chem. Phys. Lett.* **2004**, *397*, 51.
(56) Petersen, P. B.; Johnson, J. C.; Knutsen, K. P.; Saykally, R. J. *Chem. Phys. Lett.* **2004**, *397*, 46.
(57) Weber, R.; Winter, B.; Schmidt, P. M.; Widdra, W.; Hertel, I. V.; Dittmar, M.; Faubel, M. *J. Phys. Chem. B* **2004**, *108*, 4729.
(58) Winter, B.; Weber, R.; Schmidt, P. M.; Hertel, I. V.; Faubel, M.; Vrbka, L.; Jungwirth, P. *J. Phys. Chem. B* **2004**, *108*, 14558.
(59) Ghosal, S.; Shbeeb, A.; Hemminger, J. C. *Geophys. Res. Lett.* **2000**, *27*, 1879.
(60) Kang, H.; Shin, T. H.; Park, S. C.; Kim, I. K.; Han, S. J. *J. Am. Chem. Soc.* **2000**, *122*, 9842.
(61) Kim, J. H.; Shin, T.; Jung, K. H.; Kang, H. *ChemPhysChem* **2005**, *6*, 440.
(62) Borodin, A.; Hofft, O.; Kahnert, U.; Kempter, V.; Poddey, A.; Blochl, P. E. *J. Chem. Phys.* **2004**, *121*, 9671.
(63) Derjaguin, B. V. *Acta Physicochim. URS* **1941**, *14*, 633.
(64) Churaev, N. V. *Adv. Colloid Interface Sci.* **1999**, *83*, 19.
(65) Kunz, W.; Lo Nostro, P.; Ninham, B. W. *Curr. Opin. Colloid Interface Sci.* **2004**, *9*, 1.
(66) Wilson, M. A.; Pohorille, A.; Pratt, L. R. *J. Phys. Chem.* **1987**, *91*, 4873.
(67) Wilson, M. A.; Pohorille, A. *J. Chem. Phys.* **1991**, *95*, 6005.
(68) Benjamin, I. *J. Chem. Phys.* **1991**, *95*, 3698.
(69) Jungwirth, P.; Tobias, D. J. *J. Phys. Chem. B* **2002**, *106*, 6361.
(70) Perera, L.; Berkowitz, M. L. *J. Chem. Phys.* **1992**, *96*, 8288.
(71) Perera, L.; Berkowitz, M. L. *J. Chem. Phys.* **1992**, *96*, 3092.
(72) Perera, L.; Berkowitz, M. L. *J. Chem. Phys.* **1993**, *99*, 4222.
(73) Perera, L.; Berkowitz, M. L. *Z. Phys. D* **1993**, *26*, 166.
(74) Perera, L.; Berkowitz, M. L. *J. Chem. Phys.* **1993**, *99*, 4236.
(75) Perera, L.; Berkowitz, M. L. *J. Chem. Phys.* **1994**, *100*, 3085.
(76) Perera, L.; Essmann, U.; Berkowitz, M. L. *J. Chem. Phys.* **1995**, *102*, 450.

(77) Dang, L. X.; Rice, J. E.; Caldwell, J.; Kollman, P. A. *J. Am. Chem. Soc.* **1991**, *113*, 2481.

(78) Dang, L. X.; Smith, D. E. *J. Chem. Phys.* **1993**, *99*, 6950.

(79) Dang, L. X.; Garrett, B. C. *J. Chem. Phys.* **1993**, *99*, 2972.

(80) Gai, H. D.; Dang, L. X.; Schenter, G. K.; Garrett, B. C. *J. Phys. Chem.* **1995**, *99*, 13303.

(81) Gai, H. D.; Schenter, G. K.; Dang, L. X.; Garrett, B. C. *J. Chem. Phys.* **1996**, *105*, 8835.

(82) Sremaniak, L. S.; Perera, L.; Berkowitz, M. L. *Chem. Phys. Lett.* **1994**, *218*, 377.

(83) Sremaniak, L. S.; Perera, L.; Berkowitz, M. L. *J. Phys. Chem.* **1996**, *100*, 1350.

(84) Herce, D. H.; Perera, L.; Darden, T. A.; Sagui, C. *J. Chem. Phys.* **2005**, *122*, 024513.

(85) Hagberg, D.; Brdarski, S.; Karlstrom, G. *J. Phys. Chem. B* **2005**, *109*, 4111.

(86) Stuart, S. J.; Berne, B. J. *J. Phys. Chem. A* **1999**, *103*, 10300.

(87) Perera, L.; Berkowitz, M. L. *J. Chem. Phys.* **1991**, *95*, 1954.

(88) Vrbka, L.; Mucha, M.; Minofar, B.; Jungwirth, P.; Brown, E. C.; Tobias, D. J. *Curr. Opin. Colloid Interface Sci.* **2004**, *9*, 67.

(89) Markovich, G.; Giniger, R.; Levin, M.; Cheshnovsky, O. *J. Chem. Phys.* **1991**, *95*, 9416.

(90) Markovich, G.; Pollack, S.; Giniger, R.; Cheshnovsky, O. *J. Chem. Phys.* **1994**, *101*, 9344.

(91) Choi, J. H.; Kuwata, K. T.; Cao, Y. B.; Okumura, M. *J. Phys. Chem. A* **1998**, *102*, 503.

(92) Combariza, J. E.; Kestner, N. R.; Jortner, J. *Chem. Phys. Lett.* **1993**, *203*, 423.

(93) Combariza, J. E.; Kestner, N. R.; Jortner, J. *Chem. Phys. Lett.* **1994**, *221*, 156.

(94) Combariza, J. E.; Kestner, N. R.; Jortner, J. *J. Chem. Phys.* **1994**, *100*, 2851.

(95) Xantheas, S. S. *J. Phys. Chem.* **1996**, *100*, 9703.

(96) Kim, J.; Lee, H. M.; Suh, S. B.; Majumdar, D.; Kim, K. S. *J. Chem. Phys.* **2000**, *113*, 5259.

(97) Gora, R. W.; Roszak, S.; Leszczynski, J. *Chem. Phys. Lett.* **2000**, *325*, 7.

(98) Tobias, D. J.; Jungwirth, P.; Parrinello, M. *J. Chem. Phys.* **2001**, *114*, 7036.

(99) Ayala, R.; Martinez, J. M.; Pappalardo, R. R.; Marcos, E. S. *J. Chem. Phys.* **2004**, *121*, 7269.

(100) Wang, X. B.; Yang, X.; Wang, L. S.; Nicholas, J. B. *J. Chem. Phys.* **2002**, *116*, 561.

(101) Salvador, P.; Curtis, J. E.; Tobias, D. J.; Jungwirth, P. *Phys. Chem. Chem. Phys.* **2003**, *5*, 3752.

(102) Yang, X.; Kiran, B.; Wang, X. B.; Wang, L. S.; Mucha, M.; Jungwirth, P. *J. Phys. Chem. A* **2004**, *108*, 7820.

(103) Jungwirth, P.; Curtis, J. E.; Tobias, D. J. *Chem. Phys. Lett.* **2003**, *367*, 704.

(104) Wang, X. B.; Yang, X.; Nicholas, J. B.; Wang, L. S. *Science* **2001**, *294*, 1322.

(105) Yang, X.; Wang, X. B.; Wang, L. S. *J. Phys. Chem. A* **2002**, *106*, 7607.

(106) Yang, X.; Fu, Y. J.; Wang, X. B.; Slavicek, P.; Mucha, M.; Jungwirth, P.; Wang, L. S. *J. Am. Chem. Soc.* **2004**, *126*, 876.

(107) Minofar, B.; Mucha, M.; Jungwirth, P.; Yang, X.; Fu, Y. J.; Wang, X. B.; Wang, L. S. *J. Am. Chem. Soc.* **2004**, *126*, 11691.

(108) Tissandier, M. D.; Cowen, K. A.; Feng, W. Y.; Gundlach, E.; Cohen, M. H.; Earhart, A. D.; Coe, J. V.; Tuttle, T. R. *J. Phys. Chem. A* **1998**, *102*, 7787.

(109) Eigen, M. *Angew. Chem., Int. Ed. Engl.* **1964**, *3*, 1.

(110) Zundel, G. *Adv. Chem. Phys.* **2000**, *111*, 1.

(111) Agmon, N. *J. Phys. Chem. A* **2005**, *109*, 13.

(112) Pavese, M.; Berard, D. R.; Voth, G. A. *Chem. Phys. Lett.* **1999**, *300*, 93.

(113) Iyengar, S. S.; Day, T. J. F.; Voth, G. A. *Int. J. Mass Spectrom.* **2005**, *241*, 197.

(114) Shin, J. W.; Hammer, N. I.; Diken, E. G.; Johnson, M. A.; Walters, R. S.; Jaeger, T. D.; Duncan, M. A.; Christie, R. A.; Jordan, K. D. *Science* **2004**, *304*, 1137.

(115) Dang, L. X. *J. Chem. Phys.* **2003**, *119*, 6351.

(116) Petersen, M. K.; Iyengar, S. S.; Day, T. J. F.; Voth, G. A. *J. Phys. Chem. B* **2004**, *108*, 14804.

(117) Brodskaya, E.; Lyubartsev, A. P.; Laaksonen, A. *J. Phys. Chem. B* **2002**, *106*, 6479.

(118) Brodskaya, E. N.; Egorov, A. V.; Lyubartsev, A. P.; Laaksonen, A. *J. Chem. Phys.* **2003**, *119*, 10237.

(119) Robertson, W. H.; Diken, E. G.; Price, E. A.; Shin, J. W.; Johnson, M. A. *Science* **2003**, *299*, 1367.

(120) Masamura, M. *J. Comput. Chem.* **2001**, *22*, 31.

(121) Lee, H. M.; Tarkeshwar, P.; Kim, K. S. *J. Chem. Phys.* **2004**, *121*, 4657.

(122) Vegiri, A.; Shevkunov, S. V. *J. Chem. Phys.* **2000**, *113*, 8521.

(123) Essmann, U.; Perera, L.; Berkowitz, M. L.; Darden, T.; Lee, H.; Pedersen, L. G. *J. Chem. Phys.* **1995**, *103*, 8577.

(124) Yeh, I. C.; Berkowitz, M. L. *J. Chem. Phys.* **1999**, *111*, 3155.

(125) Kawata, M.; Mikami, M. *Chem. Phys. Lett.* **2001**, *340*, 157.

(126) Tyagi, S. *J. Chem. Phys.* **2005**, *122*.

(127) Tyagi, S. *Phys. Rev. E* **2004**, *70*.

(128) Brodka, A. *Chem. Phys. Lett.* **2004**, *400*, 62.

(129) Arnold, A.; Holm, C. *Comput. Phys. Commun.* **2002**, *148*, 327.

(130) Kawata, M.; Mikami, M.; Nagashima, U. *J. Chem. Phys.* **2001**, *115*, 4457.

(131) Jungwirth, P.; Tobias, D. J. *J. Phys. Chem. B* **2000**, *104*, 7702.

(132) Jungwirth, P.; Tobias, D. J. *J. Phys. Chem. B* **2001**, *105*, 10468.

(133) Dang, L. X.; Chang, T. M. *J. Phys. Chem. B* **2002**, *106*, 235.

(134) Dang, L. X. *J. Phys. Chem. B* **2002**, *106*, 10388.

(135) Mucha, M.; Frigato, T.; Levering, L. M.; Allen, H. C.; Tobias, D. J.; Dang, L. X.; Jungwirth, P. *J. Phys. Chem. B* **2005**, *109*, 7617.

(136) Jungwirth, P. Unpublished results.

(137) Nagashima, K.; Furukawa, Y. *J. Cryst. Growth* **2000**, *209*, 167.

(138) Degreve, L.; da Silva, F. L. B. *J. Chem. Phys.* **1999**, *110*, 3070.

(139) Cavallari, M.; Cavazzoni, C.; Ferrario, M. *Mol. Phys.* **2004**, *102*, 959.

(140) Zapalowski, M.; Bartczak, W. M. *Comput. Chem.* **2000**, *24*, 459.

(141) Sillanpaa, A. J.; Laasonen, K. *Phys. Chem. Chem. Phys.* **2004**, *6*, 555.

(142) Zapalowski, M.; Bartczak, W. M. *Res. Chem. Intermed.* **2001**, *27*, 855.

(143) Bartczak, W. M.; Kroh, J.; Zapalowski, M.; Pernal, K. *Philos. Trans. R. Soc. London, Ser. A: Math., Phys. Eng. Sci.* **2001**, *359*, 1593.

(144) Gopalakrishnan, S.; Jungwirth, P.; Tobias, D. J.; Allen, H. C. *J. Phys. Chem. B* **2005**, *109*, 8861.

(145) Bhatt, D.; Chee, R.; Newman, J.; Radke, C. J. *Curr. Opin. Colloid Interface Sci.* **2004**, *9*, 145.

(146) Bhatt, D.; Newman, J.; Radke, C. J. *J. Phys. Chem. B* **2004**, *108*, 9077.

(147) Petersen, P. B.; Saykally, R. J.; Mucha, M.; Jungwirth, P. *J. Phys. Chem. B* **2005**, *109*, 10915.

(148) Caldwell, J. W.; Kollman, P. A. *J. Phys. Chem.* **1995**, *99*, 6208.

(149) Dang, L. X.; Chang, T. M. *J. Chem. Phys.* **1997**, *106*, 8149.

(150) Stuart, S. J.; Berne, B. J. *J. Phys. Chem.* **1996**, *100*, 11934.

(151) Markovich, G.; Perera, L.; Berkowitz, M. L.; Cheshnovsky, O. *J. Chem. Phys.* **1996**, *105*, 2675.

(152) Burnham, C. J.; Xantheas, S. S. *J. Chem. Phys.* **2002**, *116*, 5115.

(153) Stern, H. A.; Rittner, F.; Berne, B. J.; Friesner, R. A. *J. Chem. Phys.* **2001**, *115*, 2237.

(154) Mas, E. M.; Bukowski, R.; Szalewicz, K. *J. Chem. Phys.* **2003**, *118*, 4386.

(155) Goldman, N.; Saykally, R. J. *J. Chem. Phys.* **2004**, *120*, 4777.

(156) Ren, P. Y.; Ponder, J. W. *J. Phys. Chem. B* **2003**, *107*, 5933.

(157) Grossfield, A.; Ren, P. Y.; Ponder, J. W. *J. Am. Chem. Soc.* **2003**, *125*, 15671.

(158) Tuma, L.; Jenicek, D.; Jungwirth, P. *Chem. Phys. Lett.* **2005**, *411*, 70.

(159) Tomasi, J.; Cammi, R.; Mennucci, B. *Int. J. Quantum Chem.* **1999**, *75*, 783.

(160) Dykstra, C. E. *THEOCHEM* **2001**, *573*, 63.

(161) Jungwirth, P.; Tobias, D. J. *J. Phys. Chem. A* **2002**, *106*, 379.

(162) Defay, R.; Prigogine, I.; Bellemans, A. *Surface Tension and Adsorption*; Longmans Green: London, 1966.

(163) Chattoraj, D. K.; Birdi, K. S. *Adsorption and the Gibbs Surface Excess*; Plenum: New York, 1984.

(164) Guggenheim, E. A.; Adam, N. K. *Proc. R. Soc. London, Ser. A* **1933**, *139*, 218.

(165) Rowlinson, J. S.; Widom, B. *Molecular Theory of Capilarity*; Oxford Science Publications: Oxford, 1982.

(166) Garrett, B. C. *Science* **2004**, *303*, 1146.

(167) Paluch, M. *Adv. Colloid Interface Sci.* **2000**, *84*, 27.

(168) Barraclough, C. G.; McTigue, P. T.; Ng, Y. L. *J. Electroanal. Chem.* **1992**, *329*, 9.

(169) Goh, M. C.; Hicks, J. M.; Kemnitz, K.; Pinto, G. R.; Bhattacharyya, K.; Heinz, T. F.; Eisenthal, K. B. *J. Phys. Chem.* **1988**, *92*, 5074.

(170) Du, Q.; Superfine, R.; Freysz, E.; Shen, Y. R. *Phys. Rev. Lett.* **1993**, *70*, 2313.

(171) Richmond, G. L. *Chem. Rev.* **2002**, *102*, 2693.

(172) Allen, H. C.; Raymond, E. A.; Richmond, G. L. *Curr. Opin. Colloid Interface Sci.* **2000**, *5*, 74.

(173) Wilson, K. R.; Cavalleri, M.; Rude, B. S.; Schaller, R. D.; Nilsson, A.; Pettersson, L. G. M.; Goldman, N.; Catalano, T.; Bozek, J. D.; Saykally, R. J. *J. Phys.: Condens. Matter* **2002**, *14*, L221.

(174) Matsumoto, M.; Kataoka, Y. *J. Chem. Phys.* **1988**, *88*, 3233.

(175) Pratt, L. R. *J. Phys. Chem.* **1992**, *96*, 25.

(176) Wilson, M. A.; Pohorille, A.; Pratt, L. R. *J. Chem. Phys.* **1989**, *90*, 5211.

(177) Sokhan, V. P.; Tildesley, D. J. *Mol. Phys.* **1997**, *92*, 625.

(178) Feller, S. E.; Pastor, R. W.; Rojnuckarin, A.; Bogusz, S.; Brooks, B. R. *J. Phys. Chem.* **1996**, *100*, 17011.

(179) Spicer, C. W.; Chapman, E. G.; Finlayson-Pitts, B. J.; Plastridge, R. A.; Hubbe, J. M.; Fast, J. D.; Berkowitz, C. M. *Nature* **1998**, *394*, 353.

(180) Foster, K. L.; Plastridge, R. A.; Bottenheim, J. W.; Shepson, P. B.; Finlayson-Pitts, B. J.; Spicer, C. W. *Science* **2001**, *291*, 471.

(181) Behnke, W.; Scheer, V.; Zetzsch, C. *Naturally Produced Organohalogens*; Kluwer: Dordrecht, 1995.

(182) Oum, K. W.; Lakin, M. J.; DeHaan, D. O.; Brauers, T.; Finlayson-Pitts, B. J. *Science* **1998**, *279*, 74.

(183) Roeselova, M.; Jungwirth, P.; Tobias, D. J.; Gerber, R. B. *J. Phys. Chem. B* **2003**, *107*, 12690.

(184) Knipping, E. M.; Dabdub, D. *Environ. Sci. Technol.* **2003**, *37*, 275.

(185) Hunt, S. W.; Roeselova, M.; Wang, W.; Wingen, L. M.; Knipping, E. M.; Tobias, D. J.; Dabdub, D.; Finlayson-Pitts, B. J. *J. Phys. Chem. A* **2004**, *108*, 11559.

(186) Böhm, R.; Morgner, H.; Oberbrodhage, J.; Wulf, M. *Surf. Sci.* **1994**, *317*, 407.

(187) Ghosal, S.; Hemminger, J. C.; Bluhm, H.; Mun, B. S.; Hebenstreit, E. L. D.; Ketteler, G.; Ogletree, D. F.; Requejo, F. G.; Salmeron, M. *Science* **2005**, *307*, 563.

(188) Eisenthal, K. B. *Chem. Rev.* **1996**, *96*, 1343.

(189) Corn, R. M.; Higgins, D. A. *Chem. Rev.* **1994**, *94*, 107.

(190) Miranda, P. B.; Shen, Y. R. *J. Phys. Chem. B* **1999**, *103*, 3292.

(191) Wei, X.; Shen, Y. R. *Phys. Rev. Lett.* **2001**, *86*, 4799.

(192) Morita, A.; Hynes, J. T. *Chem. Phys.* **2000**, *258*, 371.

(193) Devlin, J. P.; Joyce, C.; Buch, V. *J. Phys. Chem. A* **2000**, *104*, 1974.

(194) Buch, V. *J. Phys. Chem. B* **2005**, *109*, 17771.

(195) Benjamin, I. *Phys. Rev. Lett.* **1994**, *73*, 2083.

(196) Kuo, I. F. W.; Mundy, C. J. *Science* **2004**, *303*, 658.

(197) Morita, A.; Hynes, J. T. *J. Phys. Chem. B* **2002**, *106*, 673.

(198) Perry, A.; Ahlborn, H.; Space, B.; Moore, P. B. *J. Chem. Phys.* **2003**, *118*, 8411.

(199) Brown, E. C.; Mucha, M.; Jungwirth, P.; Tobias, D. J. *J. Phys. Chem. B* **2005**, *109*, 7934.

(200) Ferguson, D. M. *J. Comput. Chem.* **1995**, *16*, 501.

(201) Petersen, P. B.; Saykally, R. J. *J. Phys. Chem. B* **2005**, *109*, 7976.

(202) Hey, M. J.; Shield, D. W.; Speight, J. M.; Will, M. C. *J. Chem. Soc., Faraday Trans. 1* **1981**, *77*, 123.

(203) Archontis, G.; Leontidis, E.; Andreou, G. *J. Phys. Chem. B* **2005**, *109*, 17957.